International Journal of Biomathematics
(2024) 2450044 (29 pages)

DOI: 10.1142/S179352452450044X

World Scientific
www.worldscientific.com

A fractional control model to study Monkeypox transport network-related transmission

Nan Zhang[*,††], Addai Emmanuel[†,‡‡], Mary Nwaife Mezue[*], Saima Rashid[‡,§], Abiola Akinnubi[*], Zalia Abdul-Hamid[¶] and Joshua Kiddy K. Asamoah[‖,**]

[*]*School of Mathematics and Statistics*
Taiyuan Normal University
Taiyuan 030024, Shanxi, P. R. China

[†]*College of Computer and Information Science*
University of Arkansas at Little Rock
Little Rock, AR 72204, USA

[‡]*College of Mathematics, Government College University Faisalabad*
Faisalabad 38000, Pakistan

[§]*Department of Computer Science and Mathematics*
Lebanese American University
Beirut 11022801, Lebanon

[¶]*Robert H. Smith School of Business, University of Maryland*
College Park, MD 20740, USA

[‖]*Department of Mathematics, Saveetha School of Engineering*
SIMATS Chennai, India

[**]*Department of Mathematics, Kwame Nkrumah*
University of Science and Technology
Kumasi, Ghana
[††]*zhangnan1357@163.com*
[‡‡]*papayawewit@gmail.com*

Received 11 November 2023
Revised 29 February 2024
Accepted 26 March 2024
Published 29 August 2024

Communicated by Zhen Jin

Effective disease control measures to manage the spread of Monkeypox (Mpox) virus are crucial, especially given the serious public health risks posed by the ongoing global epidemic in regions where the virus is both prevalent and not. This study introduces a precise model, based on the Caputo fractional derivative, which takes into account both human and non-human populations as well as public transportation, to delve into the transmission characteristics of Mpox outbreaks. By employing the fixed point theorem, we have precisely determined the solutions regarding existence and uniqueness. We have

[††]Corresponding author.

analyzed the stability of various equilibrium states within the model to assess Mpox's transmission capabilities. Additionally, through detailed numerical simulations, we have gauged the impact of critical model parameters that contribute to enhancing Mpox prevention and management strategies. The insights gained from our research significantly enrich epidemiological understanding and lay the foundation for improved disease containment approaches.

Keywords: Monkeypox infection; Caputo fractional derivative; transport-related infection; numerical analysis and simulations.

Mathematics Subject Classification 2020: 34A08, 92D30, 93A30, 26A33, 34D20, 37M05, 92B05

1. Introduction

The COVID-19 in 2019 triggered a serious economic and health crisis for several years, and people's main efforts were focused on fighting against this infectious disease [1–5]. However, during the continuance of COVID-19, some infectious diseases occurred: the sharp increase of Monkeypox (Mpox) cases (May 2022) also needs more attention [6–8]. Mpox is a zoonotic agent that was first discovered in monkeys in the rainforests of central and western Africa, characterized by a skin rash that later develops into small blisters and scabs, and falls off after 10 days [9, 10]. The first documented case of Mpox was in a nine-month-old child from the Democratic Republic of Congo in 1970 [11]. Initially, Mpox mainly occurred in rural and remote areas of Central and West Africa. Outside of Africa, the Mpox epidemic is sporadic and affects a small number of patients [12, 13]. Between 2017 and 2023, especially in May 2022, the unexpected large outbreaks of Mpox in both endemic and non-endemic nations have recently raised severe concerns globally [14–16]. The transmission of Mpox virus from person to person includes mother-to-child vertical transmission, direct contact with infectious skin or mucosal skin lesions, respiratory droplets or indirect contact with contaminated objects or materials, and the possibility of community transmission cannot be ruled out [17, 18]. In addition to health issues, Mpox greatly affects people's lives and the world economy. The virus can be successfully transmitted from person to person, the main concern of the people and the government is to control the disease and seek effective intervention measures which are required to stop the local development of the disease and, consequently, the global Mpox outbreak [19–21].

Transportation is a critical factor in disease proliferation, enabling infected persons to move to different areas and possibly spread infection, as seen in recent pandemics like COVID-19, where international flights had a substantial role in propagating the virus [22–24]. The topic of how the Mpox virus spreads is also currently prominent among scientific discussions. To evaluate how transportation affects disease propagation, experts use mathematical strategies that factor in aspects like human concentration and rates of infection transmission. These analytical tools assist health authorities and decision-makers in applying measures such as isolations and limiting travel. Research indicated in [24], which integrated travel-associated

infection parameters into the SIS epidemic model, analyzed its influence on disease propagation. The findings highlighted that a condition for a disease to be endemic, or long-lasting, is the existence of a stable endemic state. This suggests that travel-related infections could prompt a region to experience continuous disease presence, even if it had been previously untouched by the condition. Other studies with similar insights are mentioned in [25, 26]. Nonetheless, we can mitigate the spread of disease via transportation by implementing preventative actions, including regular disinfection of commonly contacted surfaces, mandatory mask-wearing and improving air circulation within enclosed spaces.

Over the last six decades, the exploration of infectious disease dynamics has grown, evolving into an intricate, interdisciplinary field that encompasses epidemiology, public health and beyond [27, 28]. This field integrates a diverse array of scholarly disciplines such as sociology, machine learning, artificial neural networks, mathematics and biology to comprehend and forecast the transmission of diseases and other social behavioral problems [29–31]. Mathematical models play a crucial role in epidemiology, the study of disease transmission. These models utilize mathematics to describe the spread of diseases and their impact on populations. They serve as valuable tools for experimentation, allowing researchers to generate and test hypotheses, evaluate quantitative assumptions, explore specific queries, determine the sensitivity to changes in parameter values, and estimate critical parameters from data through mathematical modeling and computer simulations [32, 33].

Fractional-order differential equations offer a more accurate representation of complex systems compared to traditional integer-order models. These equations allow for the inclusion of non-integer derivatives, capturing more intricate dynamics and offering a deeper understanding of the interactions between different disease components [34–36]. By utilizing a fractional-order approach, researchers can analyze the intricate relationships between infections, considering various epidemiological parameters, immunity factors and intervention measures. Many researchers used fractional derivatives in many diseases, as shown by Akter and Jin (COVID-19) [37], Baba and Ghanbari (tuberculosis) [38], Silva and Torres (HIV) [39], Zhang *et al.* (Marburg-Mpox) [40], Ghani *et al.* (diphtheria) [41] and so on. Because fractional derivative has inheritance and memory that enable it to fully describe the dynamics of real phenomena, an analysis based on fractional derivative is more advantageous and practical. For the mathematical model of Mpox, Ngungu *et al.* [42] used real-time data to get the transmission kinetics of Mpox virus under non-drug intervention. The existence and uniqueness of solution were obtained using Krasnosel'skii fixed point theorem. In addition, sensitivity analysis of parameters based on R_0 were given. In [43], they studied a Mpox virus model using fractional calculus and the infection control policies that will help the public to better understand the significance of control parameters in the eradication. In [44], the authors established and analyzed a mathematical model of Mpox virus transmission under Caputo fractional derivative to study the effects of vaccination and environmental transmission

on the dynamics of Mpox. Peter *et al.* [45] indicated that the isolation of infected individuals in the human population, as a form of intervention to control the spread of the virus, helps reduce the transmission of the disease. In mathematical biology, the Caputo-type fractional derivative has been used in numerous epidemiological models, such as for smoking, dengue fever, Ebola and other diseases, which has unique advantages compared to other fractional derivatives [46–48].

In this paper, we build a novel insights for a nonlinear deterministic fractional-order Mpox model, encompassing new-age control interventions. This study stands out for its emphasis on infections stemming from public transportation, a factor not widely studied before. We also take into account preventative personal health measures like maintaining social distance and using disinfecting sprays in public transit settings. These prevention strategies are integrated into our model through a cutting-edge fractional optimal control methodology. Our goal is to delve into how these control strategies affect the Mpox virus dynamics by employing an original fractional-order mathematical framework. We aspire to shed light on the effectiveness of various health intervention measures, including vaccination drives, adherence to social distancing and more, in reducing the transmission risks associated with the Mpox virus in public transportation scenarios. The insights derived from our research are intended to assist decision-makers and transportation officials in crafting comprehensive health policies that tackle the spread of the disease, guaranteeing that resources are utilized appropriately and efforts are strategically directed to overcome these public health hurdles.

As for the structure of this paper, it unfolds systematically. Section 2 gives a rundown of the foundational elements of the study. Section 3 delves into the intricacies of model development. Section 4 is dedicated to basic qualitative properties of the model, where it captured the existence–uniqueness and stability of the model. Section 5 is dedicated to the numerical analysis. Section 6 encapsulates the numerical experiments and interprets the findings and finally conclusions are provided in Sec. 7.

2. Preliminaries

We give some basic lemmas, which will be used in the proof later.

Definition 2.1 ([33]). The Caputo fractional derivative of η ($\eta > 0$) order of $\mathfrak{g}$ is given by

$$ {}^{c}\mathfrak{D}_{0_+}^{\eta}\mathfrak{g}(x) = \frac{1}{\Gamma(n-\eta)}\int_0^x (x-y)^{n-\eta-1}\mathfrak{g}^{(n)}(y)\mathrm{d}y. $$

The Riemann–Liouville fractional integral of η order of $\mathfrak{g}$ is given by

$$ \mathfrak{I}_{0^+}^{\eta}\mathfrak{g}(x) = \frac{1}{\Gamma(\eta)}\int_0^x (x-y)^{\eta-1}\mathfrak{g}(y)\mathrm{d}y, $$

where $n = [\eta] + 1$, $[\eta]$ denotes the integer part of number η, provided that the right side is pointwise defined on $(0, 1)$.

Lemma 2.1 ([34]). *Assume that* $\mathfrak{u} \in C[0,T]$, *then the solution of fractional differential equation*

$$\begin{cases} {}^{c}\mathfrak{D}^{\eta}_{0_+}\mathfrak{u}(t) = \mathfrak{K}(t), \\ \mathfrak{u}(0) = \mathfrak{u}_0 \end{cases}$$

is given by

$$\mathfrak{u}(t) = \mathfrak{u}_0 + \frac{1}{\Gamma(\eta)}\int_0^x (x-y)^{\eta-1}\mathfrak{K}(y)\mathrm{d}y.$$

Lemma 2.2 (Arzelà–Ascoli theorem [35]). *Let* M *be a compact subset of* R^n, $\{\mathfrak{f}_n\}$ *be a continuous function column,* $\mathfrak{f}_n : M \to R^n$. *Assume that*

(1) $\{\mathfrak{f}_n\}$ *is uniformly bounded*: $\forall\, x \in M$, $\exists\, C > 0$, *such that* $|\{\mathfrak{f}_n\}| \leq C$;
(2) $\{\mathfrak{f}_n\}$ *is equicontinuous*: $\forall\, \varepsilon > 0$, $\exists\, \delta > 0$, *such that as* $|x-y| < \delta$, *there is* $|\mathfrak{f}_n(x) - \mathfrak{f}_n(y)| < \varepsilon$.

Then $\{\mathfrak{f}_n(x)\}$ *has convergent subsequence and uniformly converges to* $\mathfrak{f}(x)$.

Lemma 2.3 (Guo–Krasnosel'skii fixed point theorem [35]). *Let* E *be a Banach space,* $P \subset E$ *be a cone in* E. *Suppose that* Ω_1, Ω_2 *are two bounded open subsets of* U *with* $\theta \in \Omega_1, \overline{\Omega_1} \in \Omega_2$, *where* θ *is the zero element of* E. $\mathfrak{T} : P\bigcap(\overline{\Omega_2} \setminus \Omega_1) \to P$ *is a completely operator such that either*

(1) $\| \mathfrak{T}x \| \leq \| x \|, x \in P\bigcap\partial\Omega_1, \| \mathfrak{T}x \| \geq \| x \|, x \in P\bigcap\partial\Omega_2$ *or*
(2) $\| \mathfrak{T}x \| \geq \| x \|, x \in P\bigcap\partial\Omega_1, \| \mathfrak{T}x \| \leq \| x \|, x \in P\bigcap\partial\Omega_2,$

then $\mathfrak{T}$ *has at least one fixed point in* $P\bigcap(\overline{\Omega_2} \setminus \Omega_1)$.

Lemma 2.4 (Banach contraction mapping principle [36]). *Let* $\mathfrak{X}$ *be a complete metric space and define* ρ *as a distance,* $\mathfrak{S} : \mathfrak{X} \to \mathfrak{X}$. $\forall\, x, y \in \mathfrak{X}$,

$$\rho(\mathfrak{S}x, \mathfrak{S}y) \leq \theta\rho(x,y)$$

hold, where θ *is a constant that satisfies* $0 \leq \theta < 1$. *Then* $\mathfrak{S}$ *has only one fixed point on* $\mathfrak{X}$, *that is, there is a unique* $x^* \in \mathfrak{X}$ *such that* $\mathfrak{S}x^* = x^*$.

3. Model Formulation

Using a system of differential equations, we studied both human and rodent populations in a closed homogeneous environment depending on their current status with respect to the disease. The whole human and non-human population are expressed in $\mathcal{N}_{\mathfrak{h}}(t)$ and $\mathcal{N}_{\mathfrak{m}}(t)$ at any time t and are divided into eight mutually exclusive subgroups according to disease status: for non-human population: susceptible $\mathcal{S}_{\mathfrak{m}}(t)$, exposed or latent $\mathcal{E}_{\mathfrak{m}}(t)$, infected with disease symptoms $\mathcal{I}_{\mathfrak{m}}(t)$ and recovered $\mathcal{R}_{\mathfrak{m}}(t)$ while human population: susceptible $\mathcal{S}_{\mathfrak{h}}(t)$, exposed or latent $\mathcal{E}_{\mathfrak{h}}(t)$, infected with disease $\mathcal{I}_{\mathfrak{h}}(t)$ and recovered $\mathcal{R}_{\mathfrak{h}}(t)$. We introduce another compartment $\mathcal{M}(t)$ that represents the transmission of viruses and other pathogenic microorganisms in public transport. $u_1(t)$ represents practicing avoidance of rodent

Table 1. Biological significance of parameters in the model.

Parameters	Biological significance
$\Pi_{\mathfrak{h}}^{\gamma}, \Pi_{\mathfrak{m}}^{\gamma}$	The birth rate for in rodent and human
$\beta_{\mathfrak{m}}^{\gamma}$, $\beta_{\mathfrak{h}}^{\gamma}$	Contact rates from infected rodent and infected persons
$\beta_{\mathfrak{m}\mathfrak{h}}^{\gamma}$	Contact rates from infected rodent to human
$\beta_{\mathfrak{c}\mathfrak{h}}^{\gamma}$	Transmission rates in public transport
$u_{\mathfrak{m}}^{\gamma}, u_{\mathfrak{h}}^{\gamma}$	The natural mortality rate in rodent and human
$\varphi_{\mathfrak{m}}^{\gamma}(\varphi_{\mathfrak{h}}^{\gamma})$	The rate of $\mathcal{E}_{\mathfrak{m}}(\mathcal{E}_{\mathfrak{h}})$ move to $\mathcal{I}_{\mathfrak{m}}(\mathcal{I}_{\mathfrak{h}})$ in rodent (human)
$\xi_{\mathfrak{m}}^{\gamma}, \xi_{\mathfrak{h}}^{\gamma}$	The rate at which $\mathcal{I}_{\mathfrak{m}}(\mathcal{I}_{\mathfrak{h}})$ move to $\mathcal{R}_{\mathfrak{m}}(\mathcal{R}_{\mathfrak{h}})$ in rodent (human)
$\delta_{\mathfrak{m}}^{\gamma}, \delta_{\mathfrak{h}}^{\gamma}$	Disease-induced mortality rate for rodent and human
$\zeta_{\mathfrak{h}}^{\gamma}$	The rate of $\mathcal{I}_{\mathfrak{h}}$ move to $\mathcal{M}$
$m_{\mathfrak{h}}^{\gamma}$	Removal of viruses and pathogenic in public transport

touch or using rodents as pets at a time and $u_2(t)$ represents practicing physical distancing and disinfection spray in public transportation. The rest of the parameters in the models are shown in Table 1. Then the ordinary differential equations of the model (3.1) describe the dynamics of Mpox transmission incorporating public transport transmission. This specific model is as follows:

$$
\begin{cases}
\dfrac{d\mathcal{S}_{\mathfrak{m}}}{dt} = \Pi_{\mathfrak{m}} - (\mathfrak{r}_{\mathfrak{m}} + u_{\mathfrak{m}})\mathcal{S}_{\mathfrak{m}}, \\
\dfrac{d\mathcal{E}_{\mathfrak{m}}}{dt} = \mathfrak{r}_{\mathfrak{m}}\mathcal{S}_{\mathfrak{m}} - (\varphi_{\mathfrak{m}} + u_{\mathfrak{m}})\mathcal{E}_{\mathfrak{m}}, \\
\dfrac{d\mathcal{I}_{\mathfrak{m}}}{dt} = \varphi_{\mathfrak{m}}\mathcal{E}_{\mathfrak{m}} - \xi_{\mathfrak{m}}\mathcal{I}_{\mathfrak{m}} - (u_{\mathfrak{m}} + \delta_{\mathfrak{m}})\mathcal{I}_{\mathfrak{m}}, \\
\dfrac{d\mathcal{R}_{\mathfrak{m}}}{dt} = \xi_{\mathfrak{m}}\mathcal{I}_{\mathfrak{m}} - u_{\mathfrak{m}}\mathcal{R}_{\mathfrak{m}}, \\
\dfrac{d\mathcal{S}_{\mathfrak{h}}}{dt} = \Pi_{\mathfrak{h}} - (\mathfrak{r}_{\mathfrak{h}} + u_{\mathfrak{h}})\mathcal{S}_{\mathfrak{h}}, \\
\dfrac{d\mathcal{E}_{\mathfrak{h}}}{dt} = \mathfrak{r}_{\mathfrak{h}}\mathcal{S}_{\mathfrak{h}} - (\varphi_{\mathfrak{h}} + u_{\mathfrak{h}})\mathcal{E}_{\mathfrak{h}}, \\
\dfrac{d\mathcal{I}_{\mathfrak{h}}}{dt} = \varphi_{\mathfrak{h}}\mathcal{E}_{\mathfrak{h}} - (\zeta_{\mathfrak{h}} + \xi_{\mathfrak{h}} + \delta_{\mathfrak{h}} + u_{\mathfrak{h}})\mathcal{I}_{\mathfrak{h}}, \\
\dfrac{d\mathcal{R}_{\mathfrak{h}}}{dt} = \xi_{\mathfrak{h}}\mathcal{I}_{\mathfrak{h}} - u_{\mathfrak{h}}\mathcal{R}_{\mathfrak{h}}, \\
\dfrac{d\mathcal{M}}{dt} = \zeta_{\mathfrak{h}}\mathcal{I}_{\mathfrak{h}} - m_{\mathfrak{h}}\mathcal{M}, \\
\mathcal{S}_{\mathfrak{m}}(0) = \mathfrak{a}_1 \geq 0, \quad \mathcal{E}_{\mathfrak{m}}(0) = \mathfrak{a}_2 \geq 0, \quad \mathcal{I}_{\mathfrak{m}}(0) = \mathfrak{a}_3 \geq 0, \\
\mathcal{R}_{\mathfrak{m}}(0) = \mathfrak{a}_4 \geq 0, \quad \mathcal{S}_{\mathfrak{h}}(0) = \mathfrak{a}_5 \geq 0, \quad \mathcal{E}_{\mathfrak{h}}(0) = \mathfrak{a}_6 \geq 0, \\
\mathcal{I}_{\mathfrak{h}}(0) = \mathfrak{a}_7 \geq 0, \quad \mathcal{R}_{\mathfrak{h}}(0) = \mathfrak{a}_8 \geq 0, \quad \mathcal{M}(0) = \mathfrak{a}_9 \geq 0.
\end{cases}
\tag{3.1}
$$

From model (3.1), we generalize the model by considering the dynamics of the Caputo fractional differential equations. In each case, we utilized the properties of time-dimensions where, on the left-hand side, dimension is $(\text{time})^{-\gamma}$, while on the right-hand side, dimension is $(\text{time})^{-1}$, so that both sides of the equations have the same dimension. Thus, our proposed fractional-order Mpox model has the following form:

$$\begin{cases} {}^{c}\mathfrak{D}^{\gamma}_{0_+}\mathcal{S}_{\mathfrak{m}} = \Pi^{\gamma}_{\mathfrak{m}} - (\mathfrak{r}^{\gamma}_{\mathfrak{m}} + u^{\gamma}_{\mathfrak{m}})\mathcal{S}_{\mathfrak{m}}, \\ {}^{c}\mathfrak{D}^{\gamma}_{0_+}\mathcal{E}_{\mathfrak{m}} = \mathfrak{r}^{\gamma}_{\mathfrak{m}}\mathcal{S}_{\mathfrak{m}} - (\varphi^{\gamma}_{\mathfrak{m}} + u^{\gamma}_{\mathfrak{m}})\mathcal{E}_{\mathfrak{m}}, \\ {}^{c}\mathfrak{D}^{\gamma}_{0_+}\mathcal{I}_{\mathfrak{m}} = \varphi^{\gamma}_{\mathfrak{m}}\mathcal{E}_{\mathfrak{m}} - \xi^{\gamma}_{\mathfrak{m}}\mathcal{I}_{\mathfrak{m}} - (u^{\gamma}_{\mathfrak{m}} + \delta^{\gamma}_{\mathfrak{m}})\mathcal{I}_{\mathfrak{m}}, \\ {}^{c}\mathfrak{D}^{\gamma}_{0_+}\mathcal{R}_{\mathfrak{m}} = \xi^{\gamma}_{\mathfrak{m}}\mathcal{I}_{\mathfrak{m}} - u^{\gamma}_{\mathfrak{m}}\mathcal{R}_{\mathfrak{m}}, \\ {}^{c}\mathfrak{D}^{\gamma}_{0_+}\mathcal{S}_{\mathfrak{h}} = \Pi^{\gamma}_{\mathfrak{h}} - (\mathfrak{r}^{\gamma}_{\mathfrak{h}} + u^{\gamma}_{\mathfrak{h}})\mathcal{S}_{\mathfrak{h}}, \\ {}^{c}\mathfrak{D}^{\gamma}_{0_+}\mathcal{E}_{\mathfrak{h}} = \mathfrak{r}^{\gamma}_{\mathfrak{h}}\mathcal{S}_{\mathfrak{h}} - (\varphi^{\gamma}_{\mathfrak{h}} + u^{\gamma}_{\mathfrak{h}})\mathcal{E}_{\mathfrak{h}}, \\ {}^{c}\mathfrak{D}^{\gamma}_{0_+}\mathcal{I}_{\mathfrak{h}} = \varphi^{\gamma}_{\mathfrak{h}}\mathcal{E}_{\mathfrak{h}} - (\zeta^{\gamma}_{\mathfrak{h}} + \xi^{\gamma}_{\mathfrak{h}} + \delta^{\gamma}_{\mathfrak{h}} + u^{\gamma}_{\mathfrak{h}})\mathcal{I}_{\mathfrak{h}}, \\ {}^{c}\mathfrak{D}^{\gamma}_{0_+}\mathcal{R}_{\mathfrak{h}} = \xi^{\gamma}_{\mathfrak{h}}\mathcal{I}_{\mathfrak{h}} - u^{\gamma}_{\mathfrak{h}}\mathcal{R}_{\mathfrak{h}}, \\ {}^{c}\mathfrak{D}^{\gamma}_{0_+}\mathcal{M} = \zeta^{\gamma}_{\mathfrak{h}}\mathcal{I}_{\mathfrak{h}} - m^{\gamma}_{\mathfrak{h}}\mathcal{M}, \\ \mathcal{S}_{\mathfrak{m}}(0) = \mathfrak{a}_1 \geq 0, \mathcal{E}_{\mathfrak{m}}(0) = \mathfrak{a}_2 \geq 0, \mathcal{I}_{\mathfrak{m}}(0) = \mathfrak{a}_3 \geq 0, \\ \mathcal{R}_{\mathfrak{m}}(0) = \mathfrak{a}_4 \geq 0, \mathcal{S}_{\mathfrak{h}}(0) = \mathfrak{a}_5 \geq 0, \mathcal{E}_{\mathfrak{h}}(0) = \mathfrak{a}_6 \geq 0, \\ \mathcal{I}_{\mathfrak{h}}(0) = \mathfrak{a}_7 \geq 0, \mathcal{R}_{\mathfrak{h}}(0) = \mathfrak{a}_8 \geq 0, \mathcal{M}(0) = \mathfrak{a}_9 \geq 0, \end{cases} \tag{3.2}$$

where $\mathfrak{r}^{\gamma}_{\mathfrak{m}} = (\beta^{\gamma}_{\mathfrak{m}}\mathcal{I}_{\mathfrak{m}} + \beta^{\gamma}_{\mathfrak{m}\mathfrak{h}}\mathcal{I}_{\mathfrak{h}})(1-u_1)$, $\mathfrak{r}^{\gamma}_{\mathfrak{h}} = (\beta^{\gamma}_{\mathfrak{h}}\mathcal{I}_{\mathfrak{h}} + \beta^{\gamma}_{\mathfrak{e}\mathfrak{h}}\frac{M}{\sigma^{\gamma}+M} + \beta^{\gamma}_{\mathfrak{m}}\mathcal{I}_{\mathfrak{m}})(1-u_2)$, $\mathcal{N}_{\mathfrak{m}} = \mathcal{S}_{\mathfrak{m}} + \mathcal{E}_{\mathfrak{m}} + \mathcal{I}_{\mathfrak{m}} + \mathcal{R}_{\mathfrak{m}}$, $\mathcal{N}_{\mathfrak{h}} = \mathcal{S}_{\mathfrak{h}} + \mathcal{E}_{\mathfrak{h}} + \mathcal{I}_{\mathfrak{h}} + \mathcal{R}_{\mathfrak{h}}$, where ${}^{c}\mathfrak{D}^{\gamma}_{0_+}$ is Caputo fractional derivative, $0 < \gamma \leq 1$. In fact, the model (3.2) becomes (3.1) as $\gamma = 1$. The parameters of Mpox model (3.1) and (3.2) are assumed to be nonnegative numbers. The flow diagram of Mpox model is shown in Fig. 1.

Let us reformulate the proposed model (3.2) in the subsequent form:

$$\begin{cases} {}^{c}\mathfrak{D}^{\gamma}_{0_+}\mathcal{S}_{\mathfrak{m}} = \Phi_1\big(t, \mathcal{S}_{\mathfrak{m}}, \mathcal{E}_{\mathfrak{m}}, \mathcal{I}_{\mathfrak{m}}, \mathcal{R}_{\mathfrak{m}}, \mathcal{S}_{\mathfrak{h}}, \mathcal{E}_{\mathfrak{h}}, \mathcal{I}_{\mathfrak{h}}, \mathcal{R}_{\mathfrak{h}}, \mathcal{M}\big), \\ {}^{c}\mathfrak{D}^{\gamma}_{0_+}\mathcal{E}_{\mathfrak{m}} = \Phi_2\big(t, \mathcal{S}_{\mathfrak{m}}, \mathcal{E}_{\mathfrak{m}}, \mathcal{I}_{\mathfrak{m}}, \mathcal{R}_{\mathfrak{m}}, \mathcal{S}_{\mathfrak{h}}, \mathcal{E}_{\mathfrak{h}}, \mathcal{I}_{\mathfrak{h}}, \mathcal{R}_{\mathfrak{h}}, \mathcal{M}\big), \\ {}^{c}\mathfrak{D}^{\gamma}_{0_+}\mathcal{I}_{\mathfrak{m}} = \Phi_3\big(t, \mathcal{S}_{\mathfrak{m}}, \mathcal{E}_{\mathfrak{m}}, \mathcal{I}_{\mathfrak{m}}, \mathcal{R}_{\mathfrak{m}}, \mathcal{S}_{\mathfrak{h}}, \mathcal{E}_{\mathfrak{h}}, \mathcal{I}_{\mathfrak{h}}, \mathcal{R}_{\mathfrak{h}}, \mathcal{M}\big), \\ {}^{c}\mathfrak{D}^{\gamma}_{0_+}\mathcal{R}_{\mathfrak{m}} = \Phi_4\big(t, \mathcal{S}_{\mathfrak{m}}, \mathcal{E}_{\mathfrak{m}}, \mathcal{I}_{\mathfrak{m}}, \mathcal{R}_{\mathfrak{m}}, \mathcal{S}_{\mathfrak{h}}, \mathcal{E}_{\mathfrak{h}}, \mathcal{I}_{\mathfrak{h}}, \mathcal{R}_{\mathfrak{h}}, \mathcal{M}\big), \\ {}^{c}\mathfrak{D}^{\gamma}_{0_+}\mathcal{S}_{\mathfrak{h}} = \Phi_5\big(t, \mathcal{S}_{\mathfrak{m}}, \mathcal{E}_{\mathfrak{m}}, \mathcal{I}_{\mathfrak{m}}, \mathcal{R}_{\mathfrak{m}}, \mathcal{S}_{\mathfrak{h}}, \mathcal{E}_{\mathfrak{h}}, \mathcal{I}_{\mathfrak{h}}, \mathcal{R}_{\mathfrak{h}}, \mathcal{M}\big), \\ {}^{c}\mathfrak{D}^{\gamma}_{0_+}\mathcal{E}_{\mathfrak{h}} = \Phi_6\big(t, \mathcal{S}_{\mathfrak{m}}, \mathcal{E}_{\mathfrak{m}}, \mathcal{I}_{\mathfrak{m}}, \mathcal{R}_{\mathfrak{m}}, \mathcal{S}_{\mathfrak{h}}, \mathcal{E}_{\mathfrak{h}}, \mathcal{I}_{\mathfrak{h}}, \mathcal{R}_{\mathfrak{h}}, \mathcal{M}\big), \\ {}^{c}\mathfrak{D}^{\gamma}_{0_+}\mathcal{I}_{\mathfrak{h}} = \Phi_7\big(t, \mathcal{S}_{\mathfrak{m}}, \mathcal{E}_{\mathfrak{m}}, \mathcal{I}_{\mathfrak{m}}, \mathcal{R}_{\mathfrak{m}}, \mathcal{S}_{\mathfrak{h}}, \mathcal{E}_{\mathfrak{h}}, \mathcal{I}_{\mathfrak{h}}, \mathcal{R}_{\mathfrak{h}}, \mathcal{M}\big), \\ {}^{c}\mathfrak{D}^{\gamma}_{0_+}\mathcal{R}_{\mathfrak{h}} = \Phi_8\big(t, \mathcal{S}_{\mathfrak{m}}, \mathcal{E}_{\mathfrak{m}}, \mathcal{I}_{\mathfrak{m}}, \mathcal{R}_{\mathfrak{m}}, \mathcal{S}_{\mathfrak{h}}, \mathcal{E}_{\mathfrak{h}}, \mathcal{I}_{\mathfrak{h}}, \mathcal{R}_{\mathfrak{h}}, \mathcal{M}\big), \\ {}^{c}\mathfrak{D}^{\gamma}_{0_+}\mathcal{M} = \Phi_9\big(t, \mathcal{S}_{\mathfrak{m}}, \mathcal{E}_{\mathfrak{m}}, \mathcal{I}_{\mathfrak{m}}, \mathcal{R}_{\mathfrak{m}}, \mathcal{S}_{\mathfrak{h}}, \mathcal{E}_{\mathfrak{h}}, \mathcal{I}_{\mathfrak{h}}, \mathcal{R}_{\mathfrak{h}}, \mathcal{M}\big), \end{cases}$$

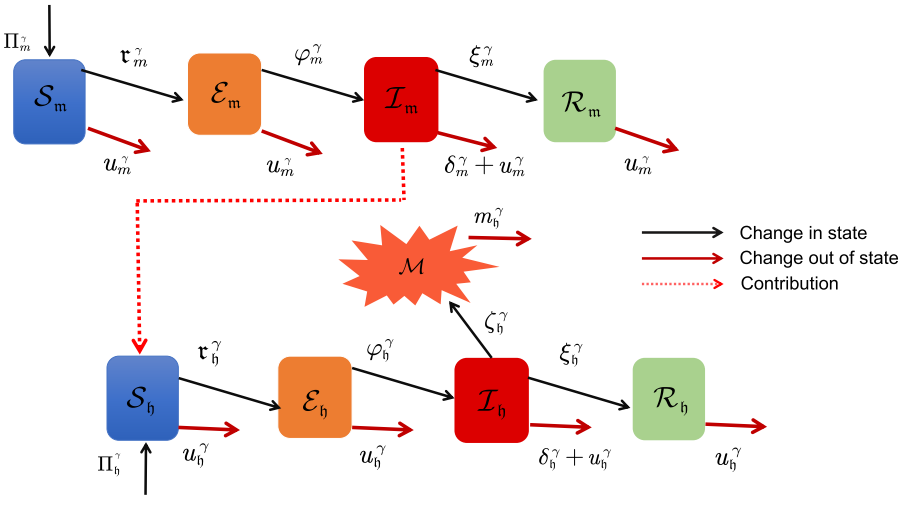

Fig. 1. Flow chart of the Mpox virus transmission.

where

$$\begin{cases}
\Phi_1\big(t,\mathcal{S}_{\mathfrak{m}},\mathcal{E}_{\mathfrak{m}},\mathcal{I}_{\mathfrak{m}},\mathcal{R}_{\mathfrak{m}},\mathcal{S}_{\mathfrak{h}},\mathcal{E}_{\mathfrak{h}},\mathcal{I}_{\mathfrak{h}},\mathcal{R}_{\mathfrak{h}},\mathcal{M}\big) = \Pi_{\mathfrak{m}}^{\gamma} - (\mathfrak{r}_{\mathfrak{m}}^{\gamma} + u_{\mathfrak{m}}^{\gamma})\mathcal{S}_{\mathfrak{m}},\\
\Phi_2\big(t,\mathcal{S}_{\mathfrak{m}},\mathcal{E}_{\mathfrak{m}},\mathcal{I}_{\mathfrak{m}},\mathcal{R}_{\mathfrak{m}},\mathcal{S}_{\mathfrak{h}},\mathcal{E}_{\mathfrak{h}},\mathcal{I}_{\mathfrak{h}},\mathcal{R}_{\mathfrak{h}},\mathcal{M}\big) = \mathfrak{r}_{\mathfrak{m}}^{\gamma}\mathcal{S}_{\mathfrak{m}} - (\varphi_{\mathfrak{m}}^{\gamma} + u_{\mathfrak{m}}^{\gamma})\mathcal{E}_{\mathfrak{m}},\\
\Phi_3\big(t,\mathcal{S}_{\mathfrak{m}},\mathcal{E}_{\mathfrak{m}},\mathcal{I}_{\mathfrak{m}},\mathcal{R}_{\mathfrak{m}},\mathcal{S}_{\mathfrak{h}},\mathcal{E}_{\mathfrak{h}},\mathcal{I}_{\mathfrak{h}},\mathcal{R}_{\mathfrak{h}},\mathcal{M}\big) = \varphi_{\mathfrak{m}}^{\gamma}\mathcal{E}_{\mathfrak{m}} - \xi_{\mathfrak{m}}^{\gamma}\mathcal{I}_{\mathfrak{m}} - (u_{\mathfrak{m}}^{\gamma} + \delta_{\mathfrak{m}}^{\gamma})\mathcal{I}_{\mathfrak{m}},\\
\Phi_4\big(t,\mathcal{S}_{\mathfrak{m}},\mathcal{E}_{\mathfrak{m}},\mathcal{I}_{\mathfrak{m}},\mathcal{R}_{\mathfrak{m}},\mathcal{S}_{\mathfrak{h}},\mathcal{E}_{\mathfrak{h}},\mathcal{I}_{\mathfrak{h}},\mathcal{R}_{\mathfrak{h}},\mathcal{M}\big) = \xi_{\mathfrak{m}}^{\gamma}\mathcal{I}_{\mathfrak{m}} - u_{\mathfrak{m}}^{\gamma}\mathcal{R}_{\mathfrak{m}},\\
\Phi_5\big(t,\mathcal{S}_{\mathfrak{m}},\mathcal{E}_{\mathfrak{m}},\mathcal{I}_{\mathfrak{m}},\mathcal{R}_{\mathfrak{m}},\mathcal{S}_{\mathfrak{h}},\mathcal{E}_{\mathfrak{h}},\mathcal{I}_{\mathfrak{h}},\mathcal{R}_{\mathfrak{h}},\mathcal{M}\big) = \Pi_{\mathfrak{h}}^{\gamma} - (\mathfrak{r}_{\mathfrak{h}}^{\gamma} + u_{\mathfrak{h}}^{\gamma})\mathcal{S}_{\mathfrak{h}},\\
\Phi_6\big(t,\mathcal{S}_{\mathfrak{m}},\mathcal{E}_{\mathfrak{m}},\mathcal{I}_{\mathfrak{m}},\mathcal{R}_{\mathfrak{m}},\mathcal{S}_{\mathfrak{h}},\mathcal{E}_{\mathfrak{h}},\mathcal{I}_{\mathfrak{h}},\mathcal{R}_{\mathfrak{h}},\mathcal{M}\big) = \mathfrak{r}_{\mathfrak{h}}^{\gamma}\mathcal{S}_{\mathfrak{h}} - (\varphi_{\mathfrak{h}}^{\gamma} + u_{\mathfrak{h}}^{\gamma})\mathcal{E}_{\mathfrak{h}},\\
\Phi_7\big(t,\mathcal{S}_{\mathfrak{m}},\mathcal{E}_{\mathfrak{m}},\mathcal{I}_{\mathfrak{m}},\mathcal{R}_{\mathfrak{m}},\mathcal{S}_{\mathfrak{h}},\mathcal{E}_{\mathfrak{h}},\mathcal{I}_{\mathfrak{h}},\mathcal{R}_{\mathfrak{h}},\mathcal{M}\big) = \varphi_{\mathfrak{h}}\mathcal{E}_{\mathfrak{h}} - (\zeta_{\mathfrak{h}} + \xi_{\mathfrak{h}} + \delta_{\mathfrak{h}} + u_{\mathfrak{h}})\mathcal{I}_{\mathfrak{h}},\\
\Phi_8\big(t,\mathcal{S}_{\mathfrak{m}},\mathcal{E}_{\mathfrak{m}},\mathcal{I}_{\mathfrak{m}},\mathcal{R}_{\mathfrak{m}},\mathcal{S}_{\mathfrak{h}},\mathcal{E}_{\mathfrak{h}},\mathcal{I}_{\mathfrak{h}},\mathcal{R}_{\mathfrak{h}},\mathcal{M}\big) = \xi_{\mathfrak{h}}^{\gamma}\mathcal{I}_{\mathfrak{h}} - u_{\mathfrak{h}}^{\gamma}\mathcal{R}_{\mathfrak{h}},\\
\Phi_9\big(t,\mathcal{S}_{\mathfrak{m}},\mathcal{E}_{\mathfrak{m}},\mathcal{I}_{\mathfrak{m}},\mathcal{R}_{\mathfrak{m}},\mathcal{S}_{\mathfrak{h}},\mathcal{E}_{\mathfrak{h}},\mathcal{I}_{\mathfrak{h}},\mathcal{R}_{\mathfrak{h}},\mathcal{M}\big) = \zeta_{\mathfrak{h}}^{\gamma}\mathcal{I}_{\mathfrak{h}} - m_{\mathfrak{h}}^{\gamma}\mathcal{M}.
\end{cases}$$

Thus, the proposed model (3.2) takes the following form:

$$\begin{cases}
{}^{c}\mathfrak{D}_{0+}^{\gamma}\mathcal{F}(t) = \mathfrak{K}(t,\mathcal{F}(t)),\\
\mathcal{F}(0) = \mathcal{F}_0 \geq 0
\end{cases}$$

on condition that

$$\mathcal{F}(t) = \big(\mathcal{S}_{\mathfrak{m}}(t),\mathcal{E}_{\mathfrak{m}}(t),\mathcal{I}_{\mathfrak{m}}(t),\mathcal{R}_{\mathfrak{m}}(t),\mathcal{S}_{\mathfrak{h}}(t),\mathcal{E}_{\mathfrak{h}}(t),\mathcal{I}_{\mathfrak{h}}(t),\mathcal{R}_{\mathfrak{h}}(t),\mathcal{M}(t)\big)^{T},$$

$$\mathcal{F}(0) = \mathcal{F}_0 = \big(\mathfrak{a}_1,\mathfrak{a}_2,\mathfrak{a}_3,\mathfrak{a}_4,\mathfrak{a}_5,\mathfrak{a}_6,\mathfrak{a}_7,\mathfrak{a}_8,\mathfrak{a}_9\big)^{T},$$

$$\mathfrak{K}(t,\mathcal{F}) = \Big(\Phi_i\big(t,\mathcal{S}_{\mathfrak{m}},\mathcal{E}_{\mathfrak{m}},\mathcal{I}_{\mathfrak{m}},\mathcal{R}_{\mathfrak{m}},\mathcal{S}_{\mathfrak{h}},\mathcal{E}_{\mathfrak{h}},\mathcal{I}_{\mathfrak{h}},\mathcal{R}_{\mathfrak{h}},\mathcal{M}\big)\Big)^{T}, \quad i = 1,2,\ldots,9.$$

In view of the properties of fractional calculus, the problem (3.2) is given by

$$\mathcal{F}(t) = \int_0^t \frac{(t-\tau)^{\gamma-1}}{\Gamma(\gamma)} \mathfrak{K}(\tau, \mathcal{F}(\tau)) \mathrm{d}\tau + \mathcal{F}_0. \tag{3.3}$$

4. Basic Qualitative Properties of the Model

4.1. *Positivity and boundedness*

Theorem 4.1. *Define the region* $\Lambda \in R_+^9$,

$$\Lambda = \left\{ \left(\mathcal{S}_{\mathfrak{m}}, \mathcal{E}_{\mathfrak{m}}, \mathcal{I}_{\mathfrak{m}}, \mathcal{R}_{\mathfrak{m}}\right) \in R_+^4, \left(\mathcal{S}_{\mathfrak{h}}, \mathcal{E}_{\mathfrak{h}}, \mathcal{I}_{\mathfrak{h}}, \mathcal{R}_{\mathfrak{h}}\right) \in R_+^4, \ \mathcal{M} \in R_+, \right.$$

$$\left. \mathcal{N}_{\mathfrak{m}} \leq \frac{\Pi_{\mathfrak{m}}^{\gamma}}{u_{\mathfrak{m}}^{\gamma}}, \ \mathcal{N}_{\mathfrak{h}} \leq \frac{\Pi_{\mathfrak{h}}^{\gamma}}{u_{\mathfrak{h}}^{\gamma}}, \ \mathcal{M} \leq \frac{\zeta_h^{\gamma} \Pi_{\mathfrak{h}}^{\gamma}}{u_{\mathfrak{h}}^{\gamma} m_{\mathfrak{h}}^{\gamma}} \right\}$$

then Λ *is positively invariant for model* (3.2) *in* R_+^9.

Proof. From the definition $\mathcal{N}_{\mathfrak{m}}$, $\mathcal{N}_{\mathfrak{h}}$ and the proposed model (3.2), it gives

$$^{c}\mathfrak{D}_{0_+}^{\gamma} \mathcal{N}_{\mathfrak{m}} = \Pi_{\mathfrak{m}}^{\gamma} - u_{\mathfrak{m}}^{\gamma} \mathcal{N}_{\mathfrak{m}} - \delta_{\mathfrak{m}}^{\gamma} \mathcal{I}_{\mathfrak{m}},$$

$$^{c}\mathfrak{D}_{0_+}^{\gamma} \mathcal{N}_{\mathfrak{h}} = \Pi_{\mathfrak{h}}^{\gamma} - u_{\mathfrak{m}}^{\gamma} \mathcal{N}_{\mathfrak{h}} - (\delta_{\mathfrak{h}}^{\gamma} + \zeta_{\mathfrak{h}}^{\gamma}) \mathcal{I}_{\mathfrak{h}},$$

then, we have

$$^{c}\mathfrak{D}_{0_+}^{\gamma} \mathcal{N}_{\mathfrak{m}} \leq \Pi_{\mathfrak{m}}^{\gamma} - u_{\mathfrak{m}}^{\gamma} \mathcal{N}_{\mathfrak{m}}, \quad {}^{c}\mathfrak{D}_{0_+}^{\gamma} \mathcal{N}_{\mathfrak{h}} \leq \Pi_{\mathfrak{h}}^{\gamma} - u_{\mathfrak{h}}^{\gamma} \mathcal{N}_{\mathfrak{h}}.$$

Using the Laplace transform and the inverse Laplace transform, one has

$$\mathcal{N}_{\mathfrak{m}}(t) \leq \mathcal{N}_{\mathfrak{m}}(0) E_{\gamma,1}(-u_{\mathfrak{m}}^{\gamma} t^{\gamma}) + \Pi_{\mathfrak{m}}^{\gamma} t^{\gamma} E_{\gamma,\gamma+1}(-u_{\mathfrak{m}}^{\gamma} t^{\gamma}),$$

$$\mathcal{N}_{\mathfrak{h}}(t) \leq \mathcal{N}_{\mathfrak{h}}(0) E_{\gamma,1}(-u_{\mathfrak{h}}^{\gamma} t^{\gamma}) + \Pi_{\mathfrak{h}}^{\gamma} t^{\gamma} E_{\gamma,\gamma+1}(-u_{\mathfrak{h}}^{\gamma} t^{\gamma}).$$

Hence, it holds that

$$\mathcal{N}_{\mathfrak{m}} \leq \frac{\Pi_{\mathfrak{m}}^{\gamma}}{u_{\mathfrak{m}}^{\gamma}}, \quad \mathcal{N}_{\mathfrak{h}} \leq \frac{\Pi_{\mathfrak{h}}^{\gamma}}{u_{\mathfrak{h}}^{\gamma}}.$$

According to $\mathcal{I}_{\mathfrak{h}} \leq \mathcal{N}_{\mathfrak{h}} \leq \frac{\Pi_{\mathfrak{h}}^{\gamma}}{u_{\mathfrak{h}}^{\gamma}}$ and ${}^{c}\mathfrak{D}_{0_+}^{\gamma} \mathcal{M} = \zeta_{\mathfrak{h}}^{\gamma} \mathcal{I}_{\mathfrak{h}} - m_{\mathfrak{h}}^{\gamma} \mathcal{M}$, one can see that

$$^{c}\mathfrak{D}_{0_+}^{\gamma} \mathcal{M} \leq \zeta_{\mathfrak{h}}^{\gamma} \frac{\Pi_{\mathfrak{h}}^{\gamma}}{u_{\mathfrak{h}}^{\gamma}} - m_{\mathfrak{h}}^{\gamma} \mathcal{M}.$$

Then, by the same method as above, we can deduce $\mathcal{M} \leq \frac{\zeta_h^{\gamma} \Pi_{\mathfrak{h}}^{\gamma}}{u_{\mathfrak{h}}^{\gamma} m_{\mathfrak{h}}^{\gamma}}$. Hence, the solution of (3.2) in Λ remains in Λ. So, the region $\Lambda \in R_+^9$ is positively invariant and attracts all the solutions in R_+^9. □

Theorem 4.2. *Under* $\mathfrak{a}_i \geq 0$ $(i = 1, 2, \ldots, 9)$, *the solution of* (3.2) *is nonnegative and bounded.*

Proof. Due to the positive of the coefficients in (3.2), we have

$$\begin{cases} {}^c\mathfrak{D}^{\gamma}_{0_+}\mathcal{S}_{\mathfrak{m}}|_{\mathcal{S}_{\mathfrak{m}}=0} = \Pi^{\gamma}_{\mathfrak{m}} > 0, \\ {}^c\mathfrak{D}^{\gamma}_{0_+}\mathcal{E}_{\mathfrak{m}}\ |_{\mathcal{E}_{\mathfrak{m}}=0} = \mathfrak{r}^{\gamma}_{\mathfrak{m}}\mathcal{S}_{\mathfrak{m}} \geq 0, \\ {}^c\mathfrak{D}^{\gamma}_{0_+}\mathcal{I}_{\mathfrak{m}}\ |_{\mathcal{I}_{\mathfrak{m}}=0} = \varphi^{\gamma}_{\mathfrak{m}}\mathcal{E}_{\mathfrak{m}} \geq 0, \\ {}^c\mathfrak{D}^{\gamma}_{0_+}\mathcal{R}_{\mathfrak{m}}\ |_{\mathcal{R}_{\mathfrak{m}}=0} = \xi^{\gamma}_{\mathfrak{m}}\mathcal{I}_{\mathfrak{m}} \geq 0, \\ {}^c\mathfrak{D}^{\gamma}_{0_+}\mathcal{S}_{\mathfrak{h}}\ |_{\mathcal{S}_{\mathfrak{h}}=0} = \Pi^{\gamma}_{\mathfrak{h}} \geq 0, \\ {}^c\mathfrak{D}^{\gamma}_{0_+}\mathcal{E}_{\mathfrak{h}}\ |_{\mathcal{E}_{\mathfrak{h}}=0} = \mathfrak{r}^{\gamma}_{\mathfrak{h}}\mathcal{S}_{\mathfrak{h}} \geq 0, \\ {}^c\mathfrak{D}^{\gamma}_{0_+}\mathcal{I}_{\mathfrak{h}}\ |_{\mathcal{I}_{\mathfrak{h}}=0} = \varphi^{\gamma}_{\mathfrak{h}}\mathcal{E}_{\mathfrak{h}} \geq 0, \\ {}^c\mathfrak{D}^{\gamma}_{0_+}\mathcal{R}_{\mathfrak{h}}\ |_{\mathcal{R}_{\mathfrak{h}}=0} = \xi^{\gamma}_{\mathfrak{h}}\mathcal{I}_{\mathfrak{h}} \geq 0, \\ {}^c\mathfrak{D}^{\gamma}_{0_+}\mathcal{M}\ |_{\mathcal{M}=0} = \zeta^{\gamma}_{\mathfrak{h}}\mathcal{I}_{\mathfrak{h}} \geq 0, \end{cases}$$

which implies that $\mathcal{S}_{\mathfrak{m}}, \mathcal{E}_{\mathfrak{m}}, \mathcal{I}_{\mathfrak{m}}, \mathcal{R}_{\mathfrak{m}}, \mathcal{S}_{\mathfrak{h}}, \mathcal{E}_{\mathfrak{h}}, \mathcal{I}_{\mathfrak{h}}, \mathcal{R}_{\mathfrak{h}}, \mathcal{M}$ are positive. According to Theorem 4.1, it gives

$$\mathcal{N}_{\mathfrak{m}}(t) \leq \mathcal{N}_{\mathfrak{m}}(0)E_{\gamma,1}(-u^{\gamma}_{\mathfrak{m}}t^{\gamma}) + \Pi^{\gamma}_{\mathfrak{m}}t^{\gamma}E_{\gamma,\gamma+1}(-u^{\gamma}_{\mathfrak{m}}t^{\gamma}),$$

$$\mathcal{N}_{\mathfrak{h}}(t) \leq \mathcal{N}_{\mathfrak{h}}(0)E_{\gamma,1}(-u^{\gamma}_{\mathfrak{h}}t^{\gamma}) + \Pi^{\gamma}_{\mathfrak{h}}t^{\gamma}E_{\gamma,\gamma+1}(-u^{\gamma}_{\mathfrak{h}}t^{\gamma}),$$

$$\mathcal{M}(t) \leq \mathcal{M}(0)E_{\gamma,1}(-m^{\gamma}_{\mathfrak{h}}t^{\gamma}) + \frac{\zeta^{\gamma}_{\mathfrak{h}}\Pi^{\gamma}_{\mathfrak{h}}}{u^{\gamma}_{\mathfrak{h}}}t^{\gamma}E_{\gamma,\gamma+1}(-m^{\gamma}_{\mathfrak{h}}t^{\gamma})$$

then from the boundedness of the above Mittag-Leffler function for any $t > 0$. Hence, we get

$$\lim_{t\to\infty}\mathcal{N}_{\mathfrak{m}}(t) = \frac{\Pi^{\gamma}_{\mathfrak{m}}}{u^{\gamma}_{\mathfrak{m}}}, \quad \lim_{t\to\infty}\mathcal{N}_{\mathfrak{h}}(t) = \frac{\Pi^{\gamma}_{\mathfrak{h}}}{u^{\gamma}_{\mathfrak{h}}}, \quad \lim_{t\to\infty}\mathcal{M}(t) = \frac{\zeta^{\gamma}_{h}\Pi^{\gamma}_{\mathfrak{h}}}{u^{\gamma}_{\mathfrak{h}}m^{\gamma}_{\mathfrak{h}}}.$$

It follow from $\mathcal{N}_{\mathfrak{m}}, \mathcal{N}_{\mathfrak{h}}, \mathcal{M}$ and $\mathcal{N}_{\mathfrak{m}} \leq \frac{\Pi^{\gamma}_{\mathfrak{m}}}{u^{\gamma}_{\mathfrak{m}}}$, $\mathcal{N}_{\mathfrak{h}} \leq \frac{\Pi^{\gamma}_{\mathfrak{h}}}{u^{\gamma}_{\mathfrak{h}}}$, $\mathcal{M} \leq \frac{\zeta^{\gamma}_{h}\Pi^{\gamma}_{\mathfrak{h}}}{u^{\gamma}_{\mathfrak{h}}m^{\gamma}_{\mathfrak{h}}}$ that the solution is bounded. □

For the basic reproduction number, let $\mathcal{H} = (\mathcal{S}_{\mathfrak{m}}, \mathcal{E}_{\mathfrak{m}}, \mathcal{I}_{\mathfrak{m}}, \mathcal{R}_{\mathfrak{m}}, \mathcal{S}_{\mathfrak{h}}, \mathcal{E}_{\mathfrak{h}}, \mathcal{I}_{\mathfrak{h}}, \mathcal{R}_{\mathfrak{h}}, \mathcal{M})^T$, some parameters of system (3.2) be

$$\mathfrak{r}_1 = \varphi^{\gamma}_{\mathfrak{m}} + u^{\gamma}_{\mathfrak{m}}, \quad \mathfrak{r}_2 = \xi^{\gamma}_{\mathfrak{m}} + u^{\gamma}_{\mathfrak{m}} + \delta^{\gamma}_{\mathfrak{m}}, \quad \mathfrak{r}_3 = \varphi^{\gamma}_{\mathfrak{h}} + u^{\gamma}_{\mathfrak{h}}, \quad \mathfrak{r}_4 = \zeta^{\gamma}_{\mathfrak{h}} + \xi^{\gamma}_{\mathfrak{h}} + \delta^{\gamma}_{\mathfrak{h}} + u^{\gamma}_{\mathfrak{h}},$$

then one observes

$$\frac{d\mathcal{H}}{dt} = F - V,$$

where

$$F(x) = \begin{bmatrix} 0 & 0 & 0 & 0 & 0 & 0 & 0 & 0 & 0 \\ 0 & 0 & \dfrac{\beta^{\gamma}_{\mathfrak{m}}(1-u_1)\Pi^{\gamma}_{\mathfrak{m}}}{u^{\gamma}_{\mathfrak{m}}} & 0 & 0 & 0 & \dfrac{\beta^{\gamma}_{\mathfrak{m}\mathfrak{h}}(1-u_1)\Pi^{\gamma}_{\mathfrak{m}}}{u^{\gamma}_{\mathfrak{m}}} & 0 & 0 \\ 0 & 0 & 0 & 0 & 0 & 0 & 0 & 0 & 0 \\ 0 & 0 & 0 & 0 & 0 & 0 & 0 & 0 & 0 \\ 0 & 0 & 0 & 0 & 0 & 0 & 0 & 0 & 0 \\ 0 & 0 & \dfrac{\beta^{\gamma}_{\mathfrak{m}}(1-u_2)\Pi^{\gamma}_{\mathfrak{h}}}{u^{\gamma}_{\mathfrak{h}}} & 0 & 0 & 0 & \dfrac{\beta^{\gamma}_{\mathfrak{h}}(1-u_2)\Pi^{\gamma}_{\mathfrak{h}}}{u^{\gamma}_{\mathfrak{h}}} & 0 & \dfrac{\beta^{\gamma}_{\mathfrak{e}\mathfrak{h}}(1-u_2)\Pi^{\gamma}_{\mathfrak{h}}}{\sigma^{\gamma}u^{\gamma}_{\mathfrak{h}}} \\ 0 & 0 & 0 & 0 & 0 & 0 & 0 & 0 & 0 \\ 0 & 0 & 0 & 0 & 0 & 0 & 0 & 0 & 0 \\ 0 & 0 & 0 & 0 & 0 & 0 & 0 & 0 & 0 \end{bmatrix},$$

$$V(x) = \begin{bmatrix} u^{\gamma}_{\mathfrak{m}} & 0 & \dfrac{\beta^{\gamma}_{\mathfrak{m}}(1-u_1)\Pi^{\gamma}_{\mathfrak{m}}}{u^{\gamma}_{\mathfrak{m}}} & 0 & 0 & 0 \\ 0 & \mathfrak{r}_1 & 0 & 0 & 0 & 0 \\ 0 & -\varphi_{\mathfrak{m}} & \mathfrak{r}_2 & 0 & 0 & 0 \\ 0 & 0 & -\xi^{\gamma}_{\mathfrak{m}} & u^{\gamma}_{\mathfrak{h}} & 0 & 0 \\ 0 & 0 & \dfrac{\beta^{\gamma}_{\mathfrak{m}}(1-u_2)\Pi^{\gamma}_{\mathfrak{h}}}{u^{\gamma}_{\mathfrak{h}}} & 0 & u^{\gamma}_{\mathfrak{h}} & 0 \\ 0 & 0 & 0 & 0 & 0 & \mathfrak{r}_3 \\ 0 & 0 & 0 & 0 & 0 & -\varphi^{\gamma}_{\mathfrak{h}} \\ 0 & 0 & 0 & 0 & 0 & 0 \\ 0 & 0 & 0 & 0 & 0 & 0 \end{bmatrix}$$

$$\begin{bmatrix} \dfrac{\beta^{\gamma}_{\mathfrak{m}\mathfrak{h}}(1-u_1)\Pi^{\gamma}_{\mathfrak{m}}}{u^{\gamma}_{\mathfrak{m}}} & 0 & 0 \\ 0 & 0 & 0 \\ 0 & 0 & 0 \\ 0 & 0 & 0 \\ \dfrac{\beta^{\gamma}_{\mathfrak{h}}(1-u_2)\Pi^{\gamma}_{\mathfrak{h}}}{u^{\gamma}_{\mathfrak{h}}} & 0 & \dfrac{\beta_{\mathfrak{e}\mathfrak{h}^{\gamma}}(1-u_2)\Pi^{\gamma\,\gamma}_{\mathfrak{h}}}{\sigma^{\gamma}u^{\gamma}_{\mathfrak{h}}} \\ 0 & 0 & 0 \\ \mathfrak{r}_4 & 0 & 0 \\ -\xi^{\gamma}_{\mathfrak{h}} & u^{\gamma}_{\mathfrak{h}} & 0 \\ -\zeta^{\gamma}_{\mathfrak{h}} & 0 & m^{\gamma}_{\mathfrak{h}} \end{bmatrix}.$$

By the definition of the basic reproduction number, we have

$$R_{0\mathfrak{m}} = \frac{\beta_{\mathfrak{m}}^{\gamma}(1-u_1)\Pi_{\mathfrak{m}}^{\gamma}\varphi_{\mathfrak{m}}^{\gamma}}{\mathfrak{r}_1\mathfrak{r}_2}, \quad R_{0\mathfrak{h}_1} = \frac{\beta_{\mathfrak{h}}^{\gamma}(1-u_2)\Pi_{\mathfrak{h}}^{\gamma}\varphi_{\mathfrak{h}}^{\gamma}}{u_{\mathfrak{h}}^{\gamma}\mathfrak{r}_3\mathfrak{r}_4},$$

$$R_{0\mathfrak{h}_2} = \frac{\beta_{\mathfrak{h}}^{\gamma}(1-u_2)\Pi_{\mathfrak{h}}^{\gamma}\varphi_{\mathfrak{h}}^{\gamma}m_{\mathfrak{h}}^{\gamma}}{u_{\mathfrak{h}}^{\gamma}\mathfrak{r}_3\mathfrak{r}_4} + \frac{\zeta_{\mathfrak{h}}^{\gamma}\varphi_{\mathfrak{h}}^{\gamma}\beta_{\mathfrak{e}\mathfrak{h}}^{\gamma}(1-u_2)\Pi_{\mathfrak{h}}^{\gamma}}{\sigma^{\gamma}u_{\mathfrak{h}}}, \quad R_{0\mathfrak{h}_3} = \frac{\beta_{\mathfrak{e}\mathfrak{h}}^{\gamma}(1-u_2)\Pi_{\mathfrak{h}}^{\gamma}\zeta_{\mathfrak{h}}^{\gamma}\varphi_{\mathfrak{h}}^{\gamma}}{\sigma^{\gamma}u_{\mathfrak{h}}^{\gamma}m_{\mathfrak{h}}^{\gamma}\mathfrak{r}_3^{\gamma}\mathfrak{r}_4^{\gamma}},$$

let $R_{0\mathfrak{h}} = \max\{R_{0\mathfrak{h}_1}, R_{0\mathfrak{h}_2}, R_{0\mathfrak{h}_3}\}$.

The disease-free equilibrium of model (3.2) is given by

$$E^0 = \left(\frac{\Pi_{\mathfrak{m}}^{\gamma}}{u_{\mathfrak{m}}^{\gamma}}, 0, 0, 0, \frac{\Pi_{\mathfrak{h}}^{\gamma}}{u_{\mathfrak{h}}^{\gamma}}, 0, 0, 0, 0, 0\right).$$

Theorem 4.3. *The disease-free equilibrium E^0 of the model (3.2) is locally asymptotically stable if $R_{0\mathfrak{m}} < 1, R_{0\mathfrak{h}} < 1$ and unstable otherwise.*

Proof. In order to obtain the stability of the disease-free equilibrium point, first obtain the determinant equation of the Jacobian matrix at the disease-free equilibrium point as follows:

$$(\lambda + u_{\mathfrak{m}})^2(\lambda + u_{\mathfrak{h}})^2[\lambda^5 + \mathfrak{b}_1\lambda^4 + \mathfrak{b}_2\lambda^3 + \mathfrak{b}_3\lambda^2 + \mathfrak{b}_4\lambda + \mathfrak{b}_5] = 0,$$

where

$$\mathfrak{b}_1 = \mathfrak{r}_1 + \mathfrak{r}_2 + \mathfrak{r}_3 + \mathfrak{r}_4 + m_{\mathfrak{h}}^{\gamma},$$

$$\mathfrak{b}_2 = \mathfrak{r}_1\mathfrak{r}_2(1 - R_{0\mathfrak{m}}) + \mathfrak{r}_3\mathfrak{r}_4(1 - R_{0\mathfrak{h}_1}) + (\mathfrak{r}_1 + \mathfrak{r}_2)(\mathfrak{r}_3 + \mathfrak{r}_4 + m_{\mathfrak{h}}) + (\mathfrak{r}_3 + \mathfrak{r}_4)m_{\mathfrak{h}}^{\gamma},$$

$$\mathfrak{b}_3 = \mathfrak{r}_1\mathfrak{r}_2(1 - R_{0\mathfrak{m}})(\mathfrak{r}_3 + \mathfrak{r}_4 + m_{\mathfrak{h}}^{\gamma}) + \mathfrak{r}_3\mathfrak{r}_4(1 - R_{0\mathfrak{h}_1})(\mathfrak{r}_1 + \mathfrak{r}_2)$$
$$+ \mathfrak{r}_3\mathfrak{r}_4m_{\mathfrak{h}}^{\gamma}(1 - R_{0\mathfrak{h}_2}) + (\mathfrak{r}_1 + \mathfrak{r}_2)(\mathfrak{r}_3 + \mathfrak{r}_4)m_{\mathfrak{h}}^{\gamma},$$

$$b_4 = \mathfrak{r}_3\mathfrak{r}_4m_{\mathfrak{h}}^{\gamma}(1 - R_{0\mathfrak{h}_2})(\mathfrak{r}_1 + \mathfrak{r}_2) + \mathfrak{r}_1\mathfrak{r}_2\mathfrak{r}_3\mathfrak{r}_4(1 - R_{0\mathfrak{m}})(1 - R_{0\mathfrak{h}_1})$$
$$+ \mathfrak{r}_1\mathfrak{r}_2(1 - R_{0\mathfrak{m}})(\mathfrak{r}_3 + \mathfrak{r}_4)m_{\mathfrak{h}}^{\gamma} + \mathfrak{r}_1\mathfrak{r}_2\mathfrak{r}_3\mathfrak{r}_4(1 - R_{0\mathfrak{h}_3}),$$

$$b_5 = \mathfrak{r}_1\mathfrak{r}_2\mathfrak{r}_3\mathfrak{r}_4m_{\mathfrak{h}}^{\gamma}(1 - R_{0\mathfrak{m}})(1 - R_{0\mathfrak{h}_2}) + \mathfrak{r}_1\mathfrak{r}_2\mathfrak{r}_3\mathfrak{r}_4m_{\mathfrak{h}}^{\gamma}(1 - R_{0\mathfrak{h}_3}).$$

There are four negative real part eigenvalues $-u_{\mathfrak{m}}^{\gamma}, -u_{\mathfrak{m}}^{\gamma}, -u_{\mathfrak{h}}^{\gamma}, -u_{\mathfrak{h}}^{\gamma}$. The coefficient $\mathfrak{b}_i$ for $i = 1, 2, \ldots, 5$ are all positive, as $R_{0\mathfrak{m}} < 1, R_{0\mathfrak{h}} < 1$, then we verify the Routh–Hurwitz condition, the disease-free equilibrium E^0 of proposed (3.2) is locally asymptotically stable if $R_{0\mathfrak{m}} < 1, R_{0\mathfrak{h}} < 1$ and is unstable otherwise. □

The discussion on endemic disease equilibrium point is mainly divided into the following situations.

Case 1. Mpox in animal infections

Let $\mathcal{S}_{\mathfrak{h}}^* = \mathcal{E}_{\mathfrak{h}}^* = \mathcal{I}_{\mathfrak{h}}^* = \mathcal{R}_{\mathfrak{h}}^* = \mathcal{M}^* = 0$, as there is animal-only Mpox. Then the endemic equilibrium is

$$E_1^* = (\mathcal{S}_{\mathfrak{m}}^*, \mathcal{E}_{\mathfrak{m}}^*, \mathcal{I}_{\mathfrak{m}}^*, \mathcal{R}_{\mathfrak{m}}^*, 0, 0, 0, 0, 0).$$

Let

$$\begin{cases} \Pi_{\mathfrak{m}}^{\gamma} - (\beta_{\mathfrak{m}}^{\gamma}(1-u_1)\mathcal{I}_{\mathfrak{m}}^* + u_{\mathfrak{m}}^{\gamma})\mathcal{S}_{\mathfrak{m}}^* = 0, \\ \beta_{\mathfrak{m}}^{\gamma}(1-u_1)\mathcal{I}_{\mathfrak{m}}^*\mathcal{S}_{\mathfrak{m}}^* - (\varphi_{\mathfrak{m}}^{\gamma} + u_{\mathfrak{m}}^{\gamma})\mathcal{E}_{\mathfrak{m}}^* = 0, \\ \varphi_{\mathfrak{m}}^{\gamma}\mathcal{E}_{\mathfrak{m}}^* - (\xi_{\mathfrak{m}}^{\gamma} + u_{\mathfrak{m}}^{\gamma} + \delta_{\mathfrak{m}}^{\gamma})\mathcal{I}_{\mathfrak{m}}^* = 0, \\ \xi_{\mathfrak{m}}^{\gamma}\mathcal{I}_{\mathfrak{m}}^* - u_{\mathfrak{m}}^{\gamma}\mathcal{R}_{\mathfrak{m}}^* = 0, \end{cases}$$

it gives

$$\mathcal{S}_{\mathfrak{m}}^* = \frac{\Pi_{\mathfrak{m}}^{\gamma}}{\beta_{\mathfrak{m}}^{\gamma}(1-u_1) + u_{\mathfrak{m}}^{\gamma}}, \quad \mathcal{E}_{\mathfrak{m}}^* = \frac{\beta_{\mathfrak{m}}^{\gamma}(1-u_1)}{(\varphi_{\mathfrak{m}}^{\gamma} + u_{\mathfrak{m}}^{\gamma})}\mathcal{S}_{\mathfrak{m}}^*,$$

$$\mathcal{I}_{\mathfrak{m}}^* = \frac{\varphi_{\mathfrak{m}}^{\gamma}}{\xi_{\mathfrak{m}}^{\gamma} + u_{\mathfrak{m}}^{\gamma} + \delta_{\mathfrak{m}}^{\gamma}}\mathcal{E}_{\mathfrak{m}}^*, \quad \mathcal{R}_{\mathfrak{m}}^* = \frac{\xi_{\mathfrak{m}}^{\gamma}}{u_{\mathfrak{m}}^{\gamma}}\mathcal{I}_{\mathfrak{m}}^*.$$

Case 2. Human-only Mpox infections

In this case, $\mathcal{S}_{\mathfrak{m}}^* = \mathcal{E}_{\mathfrak{m}}^* = \mathcal{I}_{\mathfrak{m}}^* = \mathcal{R}_{\mathfrak{m}}^* = \mathcal{M}^* = 0$, then the endemic equilibrium is

$$E_2^* = (0, 0, 0, \mathcal{S}_{\mathfrak{h}}^*, \mathcal{E}_{\mathfrak{h}}^*, \mathcal{I}_{\mathfrak{h}}^*, \mathcal{R}_{\mathfrak{h}}^*, 0).$$

Let

$$\begin{cases} \Pi_{\mathfrak{h}}^{\gamma} - (\beta_{\mathfrak{h}}^{\gamma}(1-u_2)\mathcal{I}_{\mathfrak{h}}^* + u_{\mathfrak{h}}^{\gamma})\mathcal{S}_{\mathfrak{h}}^* = 0, \\ \beta_{\mathfrak{h}}^{\gamma}(1-u_2)\mathcal{I}_{\mathfrak{h}}^*\mathcal{S}_{\mathfrak{h}}^* - (\varphi_{\mathfrak{h}}^{\gamma} + u_{\mathfrak{h}}^{\gamma})\mathcal{E}_{\mathfrak{h}}^* = 0, \\ \varphi_{\mathfrak{h}}^{\gamma}\mathcal{E}_{\mathfrak{h}}^* - (\zeta_{\mathfrak{h}}^{\gamma} + \xi_{\mathfrak{h}}^{\gamma} + \delta_{\mathfrak{h}}^{\gamma} + u_{\mathfrak{h}}^{\gamma})\mathcal{I}_{\mathfrak{h}}^* = 0, \\ \xi_{\mathfrak{h}}^{\gamma}\mathcal{I}_{\mathfrak{h}}^* - u_{\mathfrak{h}}^{\gamma}\mathcal{R}_{\mathfrak{h}}^* = 0, \end{cases}$$

we obtain

$$\mathcal{S}_{\mathfrak{h}}^* = \frac{\Pi_{\mathfrak{h}}^{\gamma}}{\beta_{\mathfrak{h}}^{\gamma}(1-u_2) + u_{\mathfrak{h}}^{\gamma}}, \quad \mathcal{E}_{\mathfrak{h}}^* = \frac{\beta_{\mathfrak{h}}^{\gamma}(1-u_2)}{(\varphi_{\mathfrak{h}}^{\gamma} + u_{\mathfrak{h}}^{\gamma})}\mathcal{S}_{\mathfrak{h}}^*,$$

$$\mathcal{I}_{\mathfrak{h}}^* = \frac{\varphi_{\mathfrak{h}}^{\gamma}}{\zeta_{\mathfrak{h}}^{\gamma} + \xi_{\mathfrak{h}}^{\gamma} + \delta_{\mathfrak{h}}^{\gamma} + u_{\mathfrak{h}}^{\gamma}}\mathcal{E}_{\mathfrak{h}}^*, \quad \mathcal{R}_{\mathfrak{h}}^* = \frac{\xi_{\mathfrak{h}}^{\gamma}}{u_{\mathfrak{h}}^{\gamma}}\mathcal{I}_{\mathfrak{h}}^*.$$

Case 3. Mpox in human and animal infections

In this case, the endemic equilibrium is

$$E_3^* = (\mathcal{S}_{\mathfrak{m}}^*, \mathcal{E}_{\mathfrak{m}}^*, \mathcal{I}_{\mathfrak{m}}^*, \mathcal{R}_{\mathfrak{m}}^*, \mathcal{S}_{\mathfrak{h}}^*, \mathcal{E}_{\mathfrak{h}}^*, \mathcal{I}_{\mathfrak{h}}^*, \mathcal{R}_{\mathfrak{h}}^*, \mathcal{M}^*).$$

Let

$$\begin{cases} \Pi_{\mathfrak{m}}^{\gamma} - (\mathfrak{r}_{\mathfrak{m}}^{\gamma} + u_{\mathfrak{m}}^{\gamma})\mathcal{S}_{\mathfrak{m}}^{*} = 0, \\ \mathfrak{r}_{\mathfrak{m}}^{\gamma}\mathcal{S}_{\mathfrak{m}}^{*} - (\varphi_{\mathfrak{m}}^{\gamma} + u_{\mathfrak{m}}^{\gamma})\mathcal{E}_{\mathfrak{m}}^{*} = 0, \\ \varphi_{\mathfrak{m}}\mathcal{E}_{\mathfrak{m}}^{*} - \xi_{\mathfrak{m}}^{\gamma}\mathcal{I}_{\mathfrak{m}}^{*} - (u_{\mathfrak{m}}^{\gamma} + \delta_{\mathfrak{m}}^{\gamma})\mathcal{I}_{\mathfrak{m}}^{*} = 0, \\ \xi_{\mathfrak{m}}^{\gamma}\mathcal{I}_{\mathfrak{m}}^{*} - u_{\mathfrak{m}}^{\gamma}\mathcal{R}_{\mathfrak{m}}^{*} = 0, \\ \Pi_{\mathfrak{h}}^{\gamma} - (\mathfrak{r}_{\mathfrak{h}}^{\gamma} + u_{\mathfrak{h}}^{\gamma})\mathcal{S}_{\mathfrak{h}}^{*} = 0, \\ \mathfrak{r}_{\mathfrak{h}}^{\gamma}\mathcal{S}_{\mathfrak{h}}^{*} - (\varphi_{\mathfrak{h}}^{\gamma} + u_{\mathfrak{h}}^{\gamma})\mathcal{E}_{\mathfrak{h}}^{*} = 0, \\ \varphi_{\mathfrak{h}}^{\gamma}\mathcal{E}_{\mathfrak{h}}^{*} - (\zeta_{\mathfrak{h}}^{\gamma} + \xi_{\mathfrak{h}}^{\gamma} + \delta_{\mathfrak{h}}^{\gamma} + u_{\mathfrak{h}}^{\gamma})\mathcal{I}_{\mathfrak{h}}^{*} = 0, \\ \xi_{\mathfrak{h}}^{\gamma}\mathcal{I}_{\mathfrak{h}}^{*} - u_{\mathfrak{h}}^{\gamma}\mathcal{R}_{\mathfrak{h}}^{*} = 0, \\ \zeta_{\mathfrak{h}}^{\gamma}\mathcal{I}_{\mathfrak{h}}^{*} - m_{\mathfrak{h}}^{\gamma}\mathcal{M}^{*} = 0, \end{cases}$$

we obtain

$$\mathcal{S}_{\mathfrak{m}}^{*} = \frac{\Pi_{\mathfrak{m}}^{\gamma}}{\mathfrak{r}_{\mathfrak{m}}^{\gamma} + u_{\mathfrak{m}}^{\gamma}}, \quad \mathcal{E}_{\mathfrak{m}}^{*} = \frac{\mathfrak{r}_{\mathfrak{m}}^{\gamma}}{(\varphi_{\mathfrak{m}}^{\gamma} + u_{\mathfrak{m}}^{\gamma})}\mathcal{S}_{\mathfrak{m}}^{*}, \quad \mathcal{I}_{\mathfrak{m}}^{*} = \frac{\varphi_{\mathfrak{m}}^{\gamma}}{\xi_{\mathfrak{m}}^{\gamma} + u_{\mathfrak{m}}^{\gamma} + \delta_{\mathfrak{m}}^{\gamma}}\mathcal{E}_{\mathfrak{m}}^{*},$$

$$\mathcal{R}_{\mathfrak{m}}^{*} = \frac{\xi_{\mathfrak{m}}^{\gamma}}{u_{\mathfrak{m}}^{\gamma}}\mathcal{I}_{\mathfrak{m}}^{*}, \quad \mathcal{S}_{\mathfrak{h}}^{*} = \frac{\Pi_{\mathfrak{h}}^{\gamma}}{\mathfrak{r}_{\mathfrak{h}}^{\gamma} + u_{\mathfrak{h}}^{\gamma}}, \quad \mathcal{E}_{\mathfrak{h}}^{*} = \frac{\mathfrak{r}_{\mathfrak{h}}^{\gamma}}{(\varphi_{\mathfrak{h}}^{\gamma} + u_{\mathfrak{h}}^{\gamma})}\mathcal{S}_{\mathfrak{h}}^{*},$$

$$\mathcal{I}_{\mathfrak{h}}^{*} = \frac{\varphi_{\mathfrak{h}}^{\gamma}}{\zeta_{\mathfrak{h}}^{\gamma} + \xi_{\mathfrak{h}}^{\gamma} + \delta_{\mathfrak{h}}^{\gamma} + u_{\mathfrak{h}}^{\gamma}}\mathcal{E}_{\mathfrak{h}}^{*}, \quad \mathcal{R}_{\mathfrak{h}}^{*} = \frac{\xi_{\mathfrak{h}}^{\gamma}}{u_{\mathfrak{h}}^{\gamma}}\mathcal{I}_{\mathfrak{h}}^{*}, \quad \mathcal{M}^{*} = \frac{\zeta_{\mathfrak{h}}^{\gamma}}{m_{\mathfrak{h}}^{\gamma}}\mathcal{I}_{\mathfrak{h}}^{*}.$$

4.2. *Existence and uniqueness of solution to model*

Let $\mathbb{B} = C([0,T];\mathbb{R})$ denote all continuous functions from $[0,T]$ to $\mathbb{R}$ endowed with the norm defined by

$$||\mathcal{F}|| = \sup_{t\in[0,T]} |\mathcal{F}(t)|,$$

where $|\mathcal{F}(t)| = |\mathcal{S}_{\mathfrak{m}}(t)| + |\mathcal{E}_{\mathfrak{m}}(t)| + |\mathcal{I}_{\mathfrak{m}}(t)| + |\mathcal{R}_{\mathfrak{m}}(t)| + |\mathcal{S}_{\mathfrak{h}}(t)| + |\mathcal{E}_{\mathfrak{h}}(t)| + |\mathcal{I}_{\mathfrak{h}}(t)| + |\mathcal{R}_{\mathfrak{h}}(t)| + |\mathcal{M}(t)|$, and $\mathcal{S}_{\mathfrak{m}}, \mathcal{E}_{\mathfrak{m}}, \mathcal{I}_{\mathfrak{m}}, \mathcal{R}_{\mathfrak{m}}, \mathcal{S}_{\mathfrak{h}}, \mathcal{E}_{\mathfrak{h}}, \mathcal{I}_{\mathfrak{h}}, \mathcal{R}_{\mathfrak{h}}, \mathcal{M} \in C[0,T]$. Let $\mathcal{V} = \{\mathcal{F} \in \mathbb{B} : |\mathcal{F}(t)| \geq 0, t \in [0,T]\}$, $\mathcal{V}_{\mathfrak{a}} = \{\mathcal{F} \in \mathbb{B} : ||\mathcal{F}|| \leq \mathfrak{a}, \mathfrak{a} > 0\}$.

Theorem 4.4. *Let* $\Phi_i\big(t, \mathcal{S}_{\mathfrak{m}}, \mathcal{E}_{\mathfrak{m}}, \mathcal{I}_{\mathfrak{m}}, \mathcal{R}_{\mathfrak{m}}, \mathcal{S}_{\mathfrak{h}}, \mathcal{E}_{\mathfrak{h}}, \mathcal{I}_{\mathfrak{h}}, \mathcal{R}_{\mathfrak{h}}, \mathcal{M}\big)$ *be continuous,* $1 < m < T$, $\mathfrak{b}_2 > \mathfrak{b}_1 > 0$, $U_0 = \max\{\mathfrak{a}_i\}$, $i = 1, 2, \ldots, 9$. *Define an operator* $\mathbf{T} : \mathcal{V} \to \mathbb{B}$ *by*

$$\mathbf{T}\mathcal{F}(t) = \int_0^t \frac{(t-\tau)^{\gamma-1}}{\Gamma(\gamma)}\mathfrak{K}(\tau, \mathcal{F}(\tau))\mathrm{d}\tau + \mathcal{F}_0, \tag{4.1}$$

and assume that

(H_1) $\Phi_i\big(t,\mathcal{S}_{\mathfrak{m}},\mathcal{E}_{\mathfrak{m}},\mathcal{I}_{\mathfrak{m}},\mathcal{R}_{\mathfrak{m}},\mathcal{S}_{\mathfrak{h}},\mathcal{E}_{\mathfrak{h}},\mathcal{I}_{\mathfrak{h}},\mathcal{R}_{\mathfrak{h}},\mathcal{M}\big) \geq \frac{\mathfrak{b}_1}{\mathfrak{N}_1}$, *for any* $\frac{1}{m} \leq t \leq m$, $0 \leq (\mathcal{S}_{\mathfrak{m}},\mathcal{E}_{\mathfrak{m}},\mathcal{I}_{\mathfrak{m}},\mathcal{R}_{\mathfrak{m}},\mathcal{S}_{\mathfrak{h}},\mathcal{E}_{\mathfrak{h}},\mathcal{I}_{\mathfrak{h}},\mathcal{R}_{\mathfrak{h}},\ \mathcal{M}) \leq (\mathfrak{b}_1,\ldots,\mathfrak{b}_1)$, *where* $\mathfrak{N}_1 = \min_{\frac{1}{m}\leq t\leq m}\int_{\frac{1}{m}}^{m}\frac{(t-\tau)^{\gamma-1}}{\Gamma(\gamma)}\mathrm{d}\tau$.

(H_2) $\Phi_i\big(t,\mathcal{S}_{\mathfrak{m}},\mathcal{E}_{\mathfrak{m}},\mathcal{I}_{\mathfrak{m}},\mathcal{R}_{\mathfrak{m}},\mathcal{S}_{\mathfrak{h}},\mathcal{E}_{\mathfrak{h}},\mathcal{I}_{\mathfrak{h}},\mathcal{R}_{\mathfrak{h}},\mathcal{M}\big) \leq \frac{\mathfrak{b}_2\Gamma(\gamma+1)}{2T^{\gamma}}$, *for any* $0 \leq t < T,\ 0 \leq (\mathcal{S}_{\mathfrak{m}},\mathcal{E}_{\mathfrak{m}},\mathcal{I}_{\mathfrak{m}},\mathcal{R}_{\mathfrak{m}},\mathcal{S}_{\mathfrak{h}},\mathcal{E}_{\mathfrak{h}},\mathcal{I}_{\mathfrak{h}},\ \mathcal{R}_{\mathfrak{h}},\mathcal{M}) \leq (\mathfrak{b}_2,\ldots,\mathfrak{b}_2)$.

Then the problem (3.2) *has at least one positive solution* U^* *with* $\mathfrak{b}_1 \leq \|U^*\| \leq \mathfrak{b}_2$.

Proof. From (4.1), we can find that $\mathbf{T}\mathcal{F} = \mathcal{F}$, i.e. the unique solution problem for considered model (3.2) change into the discussion of the fixed point of the operator $\mathcal{F}$.

Step 1. Prove that $\mathbf{T}\Psi_1$ is equicontinuous, Ψ_1 is a bounded subset of $\mathcal{V}$. Duo to $\frac{(t-\tau)^{\gamma-1}}{\Gamma(\gamma)}$ is uniformly continuous on Ψ_1. By the continuity and definition of Φ_i, there exists a constant $\mathfrak{L}_i > 0$ $(i = 1, 2, \ldots, 9)$ such that

$$0 \leq \Phi_i\big(t,\mathcal{S}_{\mathfrak{m}},\mathcal{E}_{\mathfrak{m}},\mathcal{I}_{\mathfrak{m}},\mathcal{R}_{\mathfrak{m}},\mathcal{S}_{\mathfrak{h}},\mathcal{E}_{\mathfrak{h}},\mathcal{I}_{\mathfrak{h}},\mathcal{R}_{\mathfrak{h}},\mathcal{M}\big) \leq \mathfrak{L}_i, \quad \forall\, \tau \in [0,T],\ \mathcal{F} \in \Psi_1.$$

Let $\mathfrak{L} = \max\{\mathfrak{L}_i, i = 1, 2, \ldots, 9\}$. For any $\widetilde{\varepsilon} > 0, \tau_1, \tau_2 \in [0,T]$, there exists $\widetilde{\delta} < (\frac{\Gamma(\gamma+1)\widetilde{\varepsilon}}{2\mathfrak{L}})^{\frac{1}{\gamma}},\ |\tau_2 - \tau_1| < \widetilde{\delta}$, such that

$$\Big|\frac{(\tau_2-\tau)^{\gamma-1}}{\Gamma(\gamma)} - \frac{(\tau_1-\tau)^{\gamma-1}}{\Gamma(\gamma)}\Big| < \frac{\widetilde{\varepsilon}}{2T\mathfrak{L}}.$$

For any $\mathcal{F} \in \Psi_1$, it holds that

$$\begin{aligned}|\mathbf{T}\mathcal{F}(\tau_2) - \mathbf{T}\mathcal{F}(\tau_1)| &\leq \int_0^{\tau_1}\Big|\frac{(\tau_2-\tau)^{\gamma-1}}{\Gamma(\gamma)} - \frac{(\tau_1-\tau)^{\gamma-1}}{\Gamma(\gamma)}\Big|\mathfrak{K}(\tau,\mathcal{F}(\tau))\mathrm{d}\tau \\ &\quad + \int_{\tau_1}^{\tau_2}\frac{(\tau_2-\tau)^{\gamma-1}}{\Gamma(\gamma)}\mathfrak{K}(\tau,\mathcal{F}(\tau))\mathrm{d}\tau \\ &\leq \frac{\widetilde{\varepsilon}}{2T\mathfrak{L}}T\mathfrak{L} + \frac{\widetilde{\delta}^{\gamma}\mathfrak{L}}{\Gamma(\gamma+1)} \leq \widetilde{\varepsilon},\end{aligned}$$

i.e. $\mathbf{T}\Psi_1$ is equicontinuous.

Step 2. It is shown that $\mathbf{T}\Psi_1$ is bounded. For any $\mathcal{F} \in \Psi_1$, one can see that

$$|\mathbf{T}\mathcal{F}(t)| = \Big|\int_0^t \frac{(t-\tau)^{\gamma-1}}{\Gamma(\gamma)}\mathfrak{K}(\tau,\mathcal{F}(\tau))\mathrm{d}\tau + \mathcal{F}_0\Big| \leq \frac{\mathfrak{L}T^{\gamma}}{\Gamma(\gamma+1)} + \mathcal{F}_0.$$

Thus, $\mathbf{K}\Psi_1$ is bounded.

Step 3. $\mathbf{T} : \mathcal{V} \to \mathcal{V}$ is continuous. From the continuity and nonnegativity of functions $\mathfrak{K}(\tau,\mathcal{F})$, as well as $\frac{(t-\tau)^{\gamma-1}}{\Gamma(\gamma)}$, we can deduce $\mathbf{T} : \mathcal{V} \to \mathcal{V}$. By the Lebesgue dominated convergence theorem and the continuity of $\mathfrak{K}(\tau,\mathcal{F})$, we deduce that $\mathbf{T}$ is continuous. Hence, from Steps 1–3 and by Arzelà–Ascoli theorem, $\mathbf{T} : \mathcal{V} \to \mathcal{V}$ is completely continuous.

Step 4. Obviously, $\mathbf{T} : \overline{\mathcal{V}_{\mathfrak{b}_2}} \setminus \mathcal{V}_{\mathfrak{b}_1} \to \mathcal{V}$ is a completely continuous operator. Let $U \in \mathcal{V}_{\mathfrak{b}_1}$, then $\|U\| \leq b_1$ for $t \in [0,T]$. It follows (H_1) that

$$|\mathbf{T}U(t)| = \Big| \int_0^t \frac{(t-\tau)^{\gamma-1}}{\Gamma(\gamma)} \mathfrak{K}(\tau, U(\tau)) \mathrm{d}\tau + U_0 \Big| \geq \int_{\frac{1}{m}}^m \frac{(t-\tau)^{\gamma-1}}{\Gamma(\gamma)} \mathfrak{K}(\tau, U(\tau)) \mathrm{d}\tau$$

$$\geq \mathfrak{N}_1 \frac{\mathfrak{b}_1}{\mathfrak{N}_1} \geq \mathfrak{b}_1$$

which means

$$\|\mathbf{T}U\| \geq \|U\|, \quad U \in \mathcal{V}_{\mathfrak{b}_1}.$$

Step 5. Let $U \in \mathcal{V}_{\mathfrak{b}_2}, \mathfrak{b}_2 \geq 2U_0$, then $\|U\| \leq \mathfrak{b}_2$ for $t \in [0,T]$. It follows (H_2) that

$$|\mathbf{T}U(t)| = \Big| \int_0^t \frac{(t-\tau)^{\gamma-1}}{\Gamma(\gamma)} \mathfrak{K}(\tau, U(\tau)) \mathrm{d}\tau + U_0 \Big| \leq \frac{T^\gamma}{\Gamma(\gamma+1)} \frac{\mathfrak{b}_2 \Gamma(\gamma+1)}{2T^\gamma} + \frac{\mathfrak{b}_2}{2} \leq \mathfrak{b}_2,$$

which means

$$\|\mathbf{T}U\| \leq \|U\|, \quad U \in \mathcal{V}_{\mathfrak{b}_2}.$$

Then from Guo–Krasnosel'skii fixed point theorem, we conclude that $\mathbf{T}$ has a fixed point U^* with $\mathfrak{b}_1 \leq \|U^*\| \leq \mathfrak{b}_2$, and it is clear that U^* is a positive solution of (3.2). □

Theorem 4.5. *Let* $\Phi_i\big(t, \mathcal{S}_{\mathfrak{m}}, \mathcal{E}_{\mathfrak{m}}, \mathcal{I}_{\mathfrak{m}}, \mathcal{R}_{\mathfrak{m}}, \mathcal{S}_{\mathfrak{h}}, \mathcal{E}_{\mathfrak{h}}, \mathcal{I}_{\mathfrak{h}}, \mathcal{R}_{\mathfrak{h}}, \mathcal{M}\big)$ *be continuous,* $i = 1, 2, \ldots, 9$. *Assume that*
(H_3) *for any* $\mathcal{F}_1, \mathcal{F}_2 \in \mathbb{B}$, *there exists a constant* $\mathfrak{L}_{\mathfrak{F}} > 0$, *such that*

$$|\mathfrak{K}(\tau, \mathcal{F}_1(\tau)) - \mathfrak{K}(\tau, \mathcal{F}_2(\tau))| \leq \mathfrak{L}_{\mathfrak{F}} |\mathcal{F}_1(\tau) - \mathcal{F}_2(\tau)|,$$

and let $\frac{T^\gamma \mathfrak{L}_{\mathfrak{F}}}{\Gamma(\gamma+1)} < 1$. *Then the system* (3.2) *has a unique solution.*

Proof. For any $\mathcal{F}_1, \mathcal{F}_2 \in \mathbb{B}$, by

$$|\mathfrak{K}(\tau, \mathcal{F}_1(\tau)) - \mathfrak{K}(\tau, \mathcal{F}_2(\tau))| \leq \mathfrak{L}_{\mathfrak{F}} |\mathcal{F}_1(\tau) - \mathcal{F}_2(\tau)|,$$

it gives

$$|\mathbf{T}\mathcal{F}_1(t) - \mathbf{T}\mathcal{F}_2(t)| \leq \int_0^t \frac{(t-\tau)^{\gamma-1}}{\Gamma(\gamma)} |\mathfrak{K}(\tau, \mathcal{F}_1(\tau)) - \mathfrak{K}(\tau, \mathcal{F}_2(\tau))| \mathrm{d}\tau$$

$$\leq \frac{T^\gamma}{\Gamma(\gamma+1)} \mathfrak{L}_{\mathfrak{F}} |\mathcal{F}_1(\tau) - \mathcal{F}_2(\tau)|.$$

Then we can get that

$$\|\mathbf{T}\mathcal{F}_1 - \mathbf{T}\mathcal{F}_2\| \leq \frac{T^\gamma \mathfrak{L}_{\mathfrak{F}}}{\Gamma(\gamma+1)} \|\mathcal{F}_1 - \mathcal{F}_2\|.$$

By $\frac{T^\gamma \mathfrak{L}_{\mathfrak{F}}}{\Gamma(\gamma+1)} < 1$, and contraction mapping principle, $\mathbf{T}$ has a unique fixed point, i.e. considering system (3.2) has a unique solution. □

4.3. *HU stability*

Definition 4.1 (HU stability). (H_4) If there exists a constant $\widetilde{\Omega}$, satisfying for any positive vector $\mathfrak{c} = (\mathfrak{c}_1, \mathfrak{c}_2, \ldots, \mathfrak{c}_9)^T$,

$$|{}^c\mathfrak{D}^{\gamma}_{0_+}\mathcal{F}(t) - \mathfrak{K}(t, \mathcal{F}(t))| \leq \mathfrak{c}$$

and for the unique solution $\widetilde{\mathcal{F}}$ of model (3.2) such that

$$\|\mathcal{F} - \widetilde{\mathcal{F}}\| \leq \widetilde{\Omega}\mathfrak{c},$$

then, (3.2) is HU stable.

Theorem 4.6. *Let* $\frac{T^{\gamma}\mathfrak{L}_{\mathfrak{F}}}{\Gamma(\gamma+1)} < 1$. *Assume that* (H_3) *holds and* (H_5) *there exists a function* $\Upsilon = (\Upsilon_1, \Upsilon_2, \ldots, \Upsilon_9)^T$ *such that*

$$|\Upsilon(t)| \leq \mathfrak{c}, \quad {}^c\mathfrak{D}^{\gamma}_{0_+}\mathcal{F}(t) = \mathfrak{K}(t, \mathcal{F}(t)) + \Upsilon(t).$$

Then, (3.2) *is HU stable.*

Proof. By the condition (H_5), it gives

$$\mathcal{F}(t) = \mathcal{F}_0 + \int_0^t \frac{(t-y)^{\gamma-1}}{\Gamma(\gamma)}\mathfrak{K}(y, \mathcal{F}(y))\mathrm{d}y + \int_0^t \frac{(t-y)^{\gamma-1}}{\Gamma(\gamma)}\Upsilon(y)\mathrm{d}y,$$

then we have

$$|\mathcal{F}(t) - \mathcal{F}_0 - \int_0^t \frac{(t-y)^{\gamma-1}}{\Gamma(\gamma)}\mathfrak{K}(y, \mathcal{F}(y))\mathrm{d}y| \leq \int_0^t \frac{(t-y)^{\gamma-1}}{\Gamma(\gamma)}\Upsilon(y)\mathrm{d}y = \frac{T^{\gamma}}{\Gamma(\gamma+1)}\mathfrak{c}.$$

Let $\widetilde{\mathcal{F}}$ be unique solution to system (3.2), we obtain

$$\begin{aligned}
\left|\mathcal{F}(t) - \widetilde{\mathcal{F}}(t)\right| &= \left|\mathcal{F}(t) - \widetilde{\mathcal{F}}_0 - \int_0^t \frac{(t-y)^{\eta-1}}{\Gamma(\eta)}\mathfrak{K}(y, \widetilde{\mathcal{F}}(y))\mathrm{d}y\right| \\
&\leq \left|\mathcal{F}(t) - \mathcal{F}_0 - \int_0^t \frac{(t-y)^{\gamma-1}}{\Gamma(\gamma)}\mathfrak{K}(y, \mathcal{F}(y))\mathrm{d}y\right| \\
&\quad + \int_0^t \frac{(t-y)^{\gamma-1}}{\Gamma(\gamma)}\left|\mathfrak{K}(y, \mathcal{F}(y)) - \mathfrak{K}(y, \widetilde{\mathcal{F}}(y))\right|\mathrm{d}y \\
&\leq \frac{T^{\gamma}}{\Gamma(\gamma+1)}\mathfrak{c} + \frac{T^{\gamma}\mathfrak{L}_{\mathfrak{F}}}{\Gamma(\gamma+1)}||\mathcal{F} - \widetilde{\mathcal{F}}||.
\end{aligned}$$

Thus, we get

$$\|\mathcal{F}(t) - \widetilde{\mathcal{F}}(t)\| \leq \widetilde{\Omega}\mathfrak{c},$$

where $\widetilde{\Omega} = \frac{T^{\gamma}}{\Gamma(\gamma+1) - T^{\gamma}\mathfrak{L}_{\mathfrak{F}}}$. Hence, by the (H_4) of Definition 4.1, the system (3.2) is HU stable. □

5. Numerical Method

In this section, we use Corrector–Predictor iterative algorithm to obtain numerical solution of the model (3.2). Consider the step length $\mathfrak{h} = \frac{T}{\mathfrak{L}}$, we divide the interval $[0, T]$, $t_0 = 0, t_{\mathfrak{k}+1} = t_{\mathfrak{k}} + \mathfrak{h}, \mathfrak{k} = 0, 1, 2, \ldots, \mathfrak{L} - 1, t_{\mathfrak{L}} = T$. Suppose we have already calculated the approximations $\mathcal{F}_a(t_{\mathfrak{k}}) \approx \mathcal{F}(t_{\mathfrak{k}}), \mathfrak{k} = 0, 1, \ldots, m$, then $\mathcal{F}_a(t_{m+1})$ can be calculated using the integral equation equivalent to system (3.2),

$$\mathcal{F}_a(t_{m+1}) = \frac{\mathfrak{h}^{\eta}}{\Gamma(\eta+2)} \left[\sum_{\mathfrak{k}=0}^{m} h_{\mathfrak{k},m+1} \mathfrak{K}(t_{\mathfrak{k}}, \mathcal{F}_a(t_{\mathfrak{k}})) + \mathfrak{K}(t_{m+1}, \mathcal{F}_a^p(t_{m+1})) \right] + \mathcal{F}_0,$$

where

$$h_{\mathfrak{k},m+1} = \begin{cases} m^{\eta+1} - (m-\eta)(m+1)^{\eta}, & \mathfrak{k} = 0, \\ (m-\mathfrak{k}+2)^{\eta+1} + (m-\mathfrak{k})^{\eta+1} - 2(m-\mathfrak{k}+1)^{\eta+1}, & 1 \le \mathfrak{k} \le m, \\ 1, & \mathfrak{k} = m+1. \end{cases}$$

The Predictor formula is derived as follows:

$$\mathcal{F}_a^p(t_{m+1}) = \frac{1}{\Gamma(\gamma)} \sum_{\mathfrak{k}=0}^{m} c_{\mathfrak{k},m+1} \mathfrak{K}(t_{\mathfrak{k}}, \mathcal{F}_a(t_{\mathfrak{k}})) + \mathcal{F}_0,$$

where

$$c_{\mathfrak{k},m+1} = \frac{\mathfrak{h}^{\eta}}{\eta} [(m-\mathfrak{k}+1)^{\gamma} - (m-\mathfrak{k})^{\gamma}].$$

Let $\mathcal{W}_i(t, \mathcal{F}) = \Phi_i\big(t, \mathcal{S}_{\mathfrak{m}}, \mathcal{E}_{\mathfrak{m}}, \mathcal{I}_{\mathfrak{m}}, \mathcal{R}_{\mathfrak{m}}, \mathcal{S}_{\mathfrak{h}}, \mathcal{E}_{\mathfrak{h}}, \mathcal{I}_{\mathfrak{h}}, \mathcal{R}_{\mathfrak{h}}, \mathcal{M}\big),\ i = 1, 2, \ldots, 9$. Thus, the corrector formula for the projected model (3.2) is

$$\mathcal{S}_{\mathfrak{m}}(t_{m+1}) = \frac{\mathfrak{h}^{\gamma}}{\Gamma(\gamma+2)} \left[\sum_{\mathfrak{k}=0}^{m} h_{\mathfrak{k},m+1} \mathcal{W}_1(t_{\mathfrak{k}}, \mathcal{F}_a(t_{\mathfrak{k}})) + \mathcal{W}_1(t_{m+1}, \mathcal{F}_a^p(t_{m+1})) \right] + \mathfrak{a}_1,$$

$$\mathcal{E}_{\mathfrak{m}}(t_{m+1}) = \frac{\mathfrak{h}^{\gamma}}{\Gamma(\gamma+2)} \left[\sum_{\mathfrak{k}=0}^{m} h_{\mathfrak{k},m+1} \mathcal{W}_2(t_{\mathfrak{k}}, \mathcal{F}_a(t_{\mathfrak{k}})) + \mathcal{W}_2(t_{m+1}, \mathcal{F}_a^p(t_{m+1})) \right] + \mathfrak{a}_2,$$

$$\mathcal{I}_{\mathfrak{m}}(t_{m+1}) = \frac{\mathfrak{h}^{\gamma}}{\Gamma(\gamma+2)} \left[\sum_{\mathfrak{k}=0}^{m} h_{\mathfrak{k},m+1} \mathcal{W}_3(t_{\mathfrak{k}}, \mathcal{F}_a(t_{\mathfrak{k}})) + \mathcal{W}_3(t_{m+1}, \mathcal{F}_a^p(t_{m+1})) \right] + \mathfrak{a}_3,$$

$$\mathcal{R}_{\mathfrak{m}}(t_{m+1}) = \frac{\mathfrak{h}^{\gamma}}{\Gamma(\gamma+2)} \left[\sum_{\mathfrak{k}=0}^{m} h_{\mathfrak{k},m+1} \mathcal{W}_4(t_{\mathfrak{k}}, \mathcal{F}_a(t_{\mathfrak{k}})) + \mathcal{W}_4(t_{m+1}, \mathcal{F}_a^p(t_{m+1})) \right] + \mathfrak{a}_4,$$

$$\mathcal{S}_{\mathfrak{h}}(t_{m+1}) = \frac{\mathfrak{h}^{\gamma}}{\Gamma(\gamma+2)} \left[\sum_{\mathfrak{k}=0}^{m} h_{\mathfrak{k},m+1} \mathcal{W}_5(t_{\mathfrak{k}}, \mathcal{F}_a(t_{\mathfrak{k}})) + \mathcal{W}_5(t_{m+1}, \mathcal{F}_a^p(t_{m+1})) \right] + \mathfrak{a}_5,$$

$$\mathcal{E}_{\mathfrak{h}}(t_{m+1}) = \frac{\mathfrak{h}^{\gamma}}{\Gamma(\gamma+2)} \left[\sum_{\mathfrak{k}=0}^{m} h_{\mathfrak{k},m+1} \mathcal{W}_6(t_{\mathfrak{k}}, \mathcal{F}_a(t_{\mathfrak{k}})) + \mathcal{W}_6(t_{m+1}, \mathcal{F}_a^p(t_{m+1})) \right] + \mathfrak{a}_6,$$

$$\mathcal{I}_{\mathfrak{h}}(t_{m+1}) = \frac{\mathfrak{h}^{\gamma}}{\Gamma(\gamma+2)}\left[\sum_{\mathfrak{k}=0}^{m} h_{\mathfrak{k},m+1}\mathcal{W}_7(t_{\mathfrak{k}},\mathcal{F}_a(t_{\mathfrak{k}})) + \mathcal{W}_7(t_{m+1},\mathcal{F}_a^p(t_{m+1}))\right] + \mathfrak{a}_7,$$

$$\mathcal{R}_{\mathfrak{h}}(t_{m+1}) = \frac{\mathfrak{h}^{\gamma}}{\Gamma(\gamma+2)}\left[\sum_{\mathfrak{k}=0}^{m} h_{\mathfrak{k},m+1}\mathcal{W}_8(t_{\mathfrak{k}},\mathcal{F}_a(t_{\mathfrak{k}})) + \mathcal{W}_8(t_{m+1},\mathcal{F}_a^p(t_{m+1}))\right] + \mathfrak{a}_8,$$

$$\mathcal{M}(t_{m+1}) = \frac{\mathfrak{h}^{\gamma}}{\Gamma(\gamma+2)}\left[\sum_{\mathfrak{k}=0}^{m} h_{\mathfrak{k},m+1}\mathcal{W}_9(t_{\mathfrak{k}},\mathcal{F}_a(t_{\mathfrak{k}})) + \mathcal{W}_9(t_{m+1},\mathcal{F}_a^p(t_{m+1}))\right] + \mathfrak{a}_9.$$

6. Numerical Simulation and Discussion

This section of the study presents the fractional-order models numerical techniques to understand the behavior of the solution trajectories better. We compute the model associated with the Caputo fractional operator $\gamma \in (0.1)$ using the fractional Predictor–Corrector technique to gain insight into the solution trajectories. For this, we start with initial values for each compartment in the fractional-order model we have suggested: $\mathcal{S}_{\mathfrak{m}} = 500,\ \mathcal{E}_{\mathfrak{m}} = 400,\ \mathcal{I}_{\mathfrak{m}} = 350,\ \mathcal{R}_{\mathfrak{m}} = 200,\ \mathcal{S}_{\mathfrak{h}} = 1000,\ \mathcal{E}_{\mathfrak{h}} = 300,\ \mathcal{I}_{\mathfrak{h}} = 150,\ \mathcal{R}_{\mathfrak{h}} = 50,\ \mathcal{R} = 250$. We compare the effects of various fractional-order values with of a step size 0.2 throughout the time range $[0, 500]$ against the parameter values listed in Table 2 on both non-human and human populations. Figures 2 and 3 show dynamics of reproduction number and the sensitivity analysis of the various reproduction numbers obtained from the proposed model. It is noticed that an increase in the various transmission rate increases the number of secondary infections in both compartments. From Figs. 3(a) and 3(b), it is noticed that an increase in the control parameter (personal protection measures, $u_1(t)$) and hydro-alcoholic gel and hand-washing with soap and disinfection spray at a time, that is $u_2(t)$, has a negative correlation with the reproduction number. Interestingly, the behavior of both populations are affected by changing the order of the fractional derivative, we observed distinct memory effects in each, as shown in Figs. 4 and 5. We observed an increase in the number of susceptible rodents, exposed and infected rodents, that is Figs. 4(a)–4(c). This dynamics can be attributed to the direct relationship between exposed and infected rodents. Similarly, Figs. 5(b)–5(d)

Table 2. Parameter values in the model.

Parameters	Value	Parameters	Value
$\Pi_{\mathfrak{h}}^{\gamma}, \Pi_{\mathfrak{m}}^{\gamma}$	100; 1000	$u_{\mathfrak{h}}^{\gamma}$	1/100
$\varphi_{\mathfrak{h}}^{\gamma}$	0.05	$\xi_{\mathfrak{h}}^{\gamma}$	0.046
$\delta_{\mathfrak{h}}^{\gamma}$	0.00002	$\zeta_{\mathfrak{h}}^{\gamma}$	0.019
$m_{\mathfrak{h}}^{\gamma}$	0.00003	μ_m^{γ}	0.0020
$\beta_{\mathfrak{h}}^{\gamma}$	0.0001	$\beta_{\mathfrak{e}\mathfrak{h}}^{\gamma}$	0.0061
$\beta_{\mathfrak{m}\mathfrak{h}}^{\gamma}$	0.000041	σ^{γ}	0.4
$\beta_{\mathfrak{m}}^{\gamma}$	0.000009	$\delta_{\mathfrak{m}}^{\gamma}$	0.00002
$\xi_{\mathfrak{m}}^{\gamma}$	0.01	$\varphi_{\mathfrak{m}}^{\gamma}$	0.0076

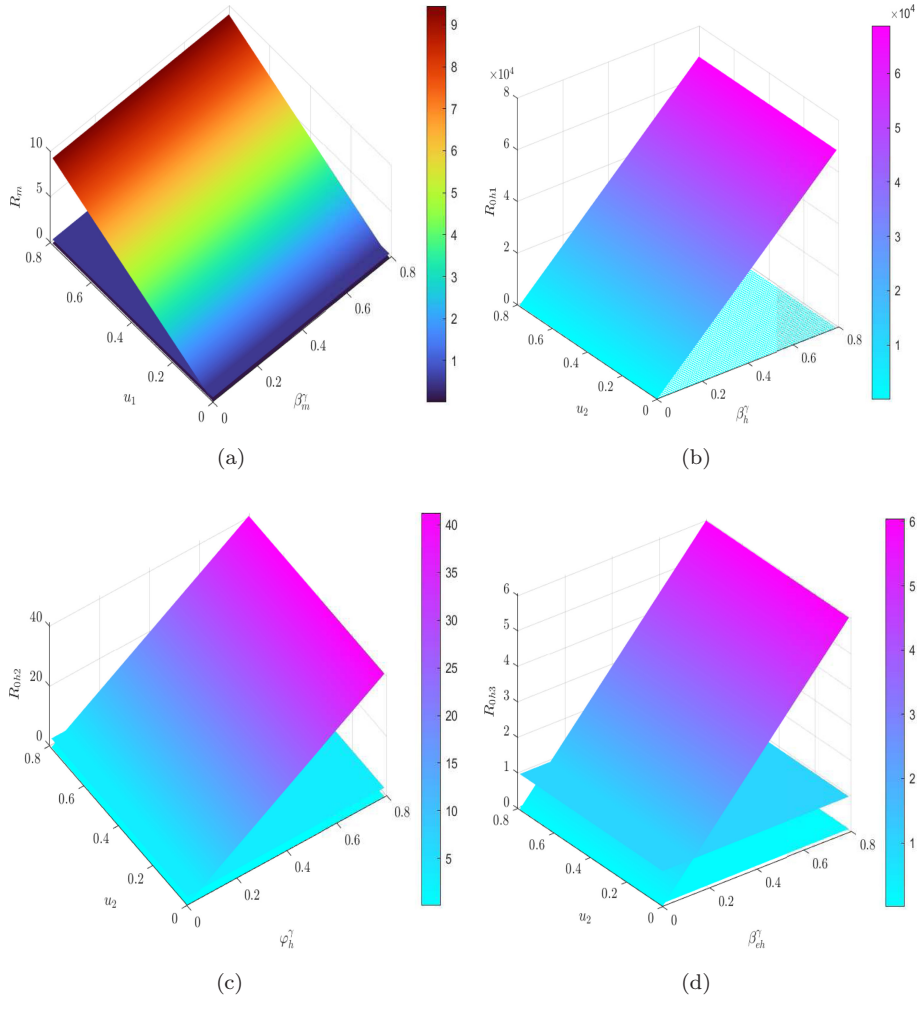

Fig. 2. Dynamics of reproduction number of the Mpox model. (a) $R_{0\mathfrak{m}}$ against β_m^γ and u_1, (b) $R_{0\mathfrak{h}_1}$ against β_h^γ and u_2, (c) $R_{0\mathfrak{h}_2}$ against φ_h^γ and u_2, (d) $R_{0\mathfrak{h}_3}$ against β_{eh}^γ and u_2.

exhibit direct relationship between exposed, infectious and recovery individuals to Mpox infection. In biological perspective, these trajectories show that whenever the population is highly exposed to the virus or disease, the probability of getting infected is possibly high and vice versa. These graphs in Figs. 6(a)–6(e) demonstrate how dependence the system is on the history of the Mpox and how sensitive it is to vary the fractional-order value. Next, we investigate the impact of control strategies on the transmission dynamics of our proposed model in both human and rodent population. The applied control interventions are described as follows:

(1) Apply the use of personal protection measures to prevent rodent touch or avoid using rodents as pets at a time, that is $u_1(t)$.

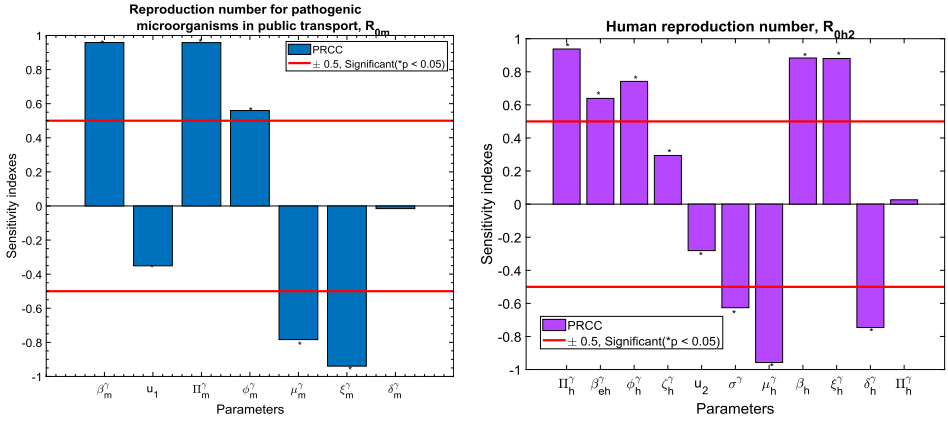

(a) (b)

Fig. 3. Latin hypercube sampling plot (sensitivity analysis) of the reproduction numbers. (a) The reproduction numbers for pathogenic microorganisms in public transport, $R_{0\mathrm{m}}$. (b) The reproduction numbers for human transmission, $R_{\mathrm{o},\mathrm{h}2}$.

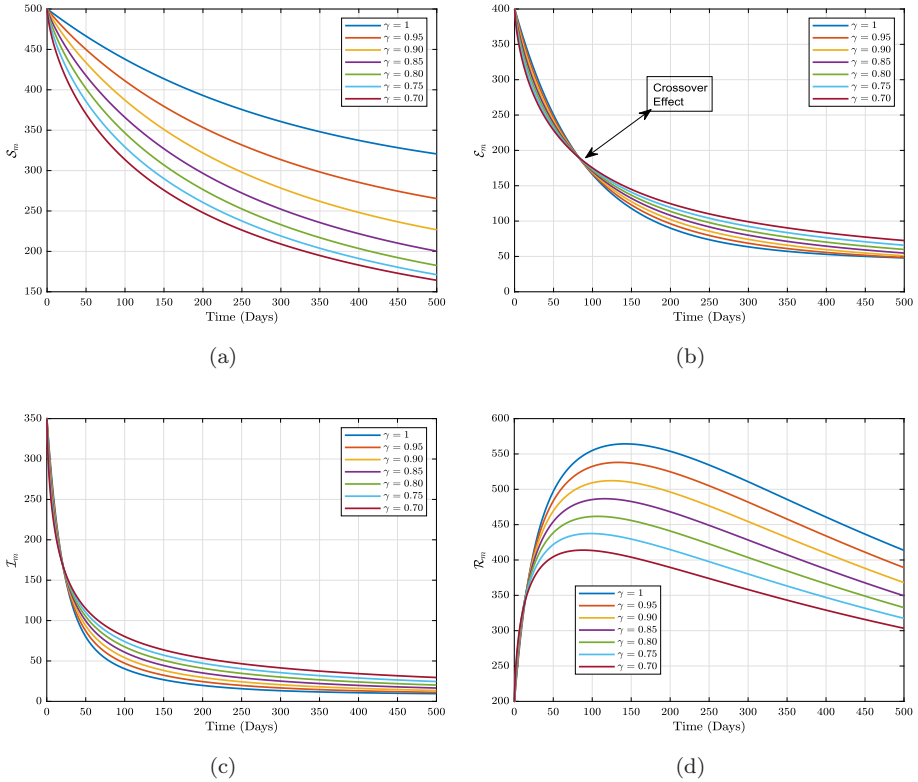

(a) (b)

(c) (d)

Fig. 4. Dynamics of rodent population at different fractional-order α. The time series plots for (a) susceptible $\mathcal{S}_{\mathrm{m}}$, (b) exposed or latent $\mathcal{E}_{\mathrm{m}}$, (c) infected $\mathcal{I}_{\mathrm{m}}$, (d) recovered $\mathcal{R}_{\mathrm{m}}$ in model (3.2) when fractional-order values $\gamma = 1$, $\gamma = 0.95$, $\gamma = 0.90$, $\gamma = 0.85$, $\gamma = 0.80$.

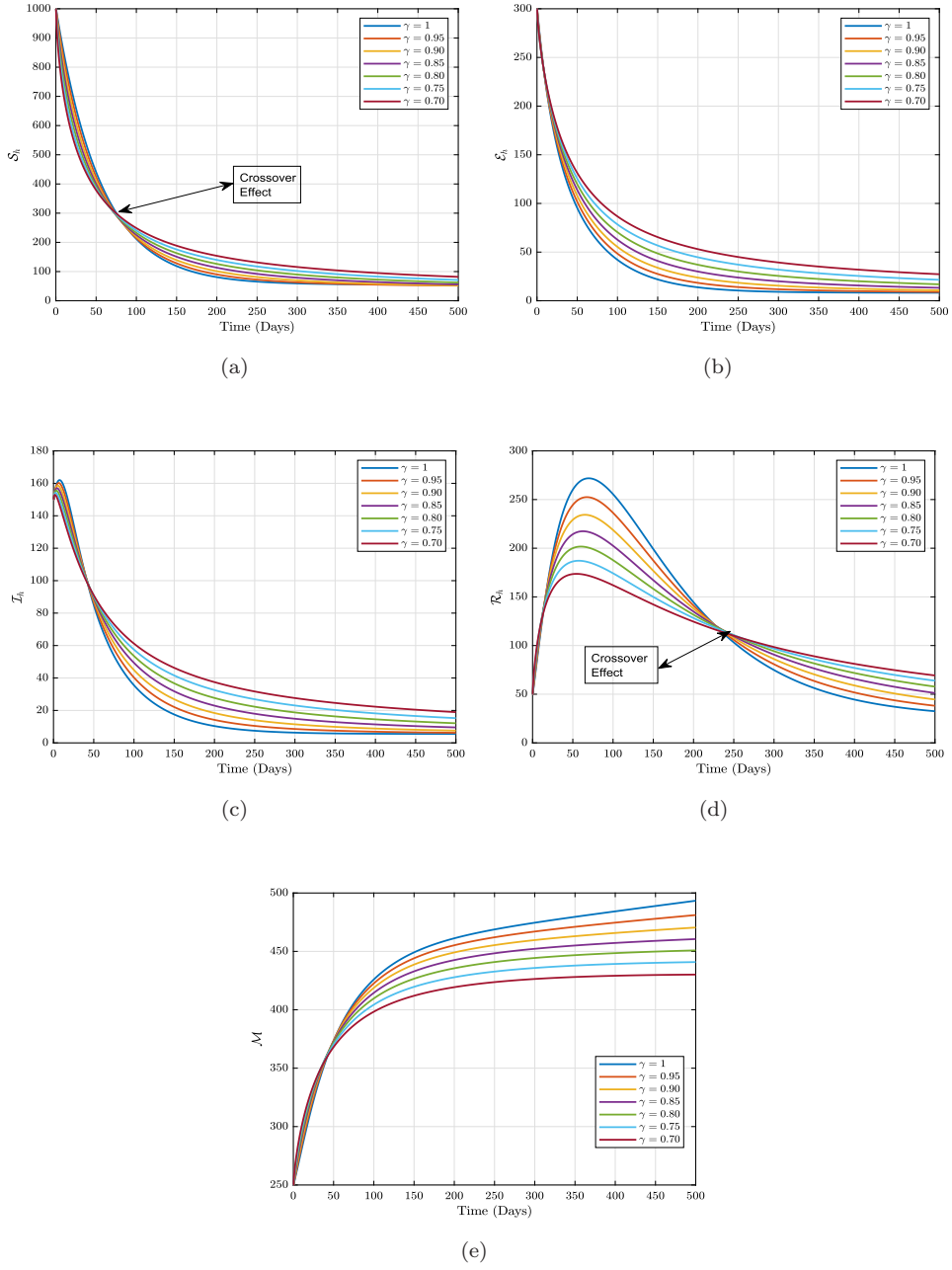

Fig. 5. Dynamics of human population at different fractional-order α. The time series plots for (a) susceptible $\mathcal{S}_\mathfrak{h}$, (b) exposed or latent $\mathcal{E}_\mathfrak{h}$, (c) infected $\mathcal{I}_\mathfrak{h}$, (d) recovered $\mathcal{R}_\mathfrak{h}$, (e) $\mathcal{M}$ in model (3.2) when fractional-order values $\gamma = 1$, $\gamma = 0.95$, $\gamma = 0.90$, $\gamma = 0.85$, $\gamma = 0.80$.

(2) Apply the use of personal protection measures to protect oneself in public transportation such as the use of hydro-alcoholic gel and hand-washing with soap and disinfection spray at a time, that is $u_2(t)$.
(3) Apply combination of personal protection measures to prevent or protect oneself again rodent touch or avoid using rodents as pets and disinfection spray in transportation at a time, that is $u_1(t)$ and $u_2(t)$.

Strategy 1, which is Fig. 6, is used to optimize Mpox disease transmission dynamics while neglecting the personal protection measures to protect oneself in public transport at a time, $u_2(t)$. We observed a decrease in the number of exposed and infection in human population and interestingly, a minimal or no effect in human population.

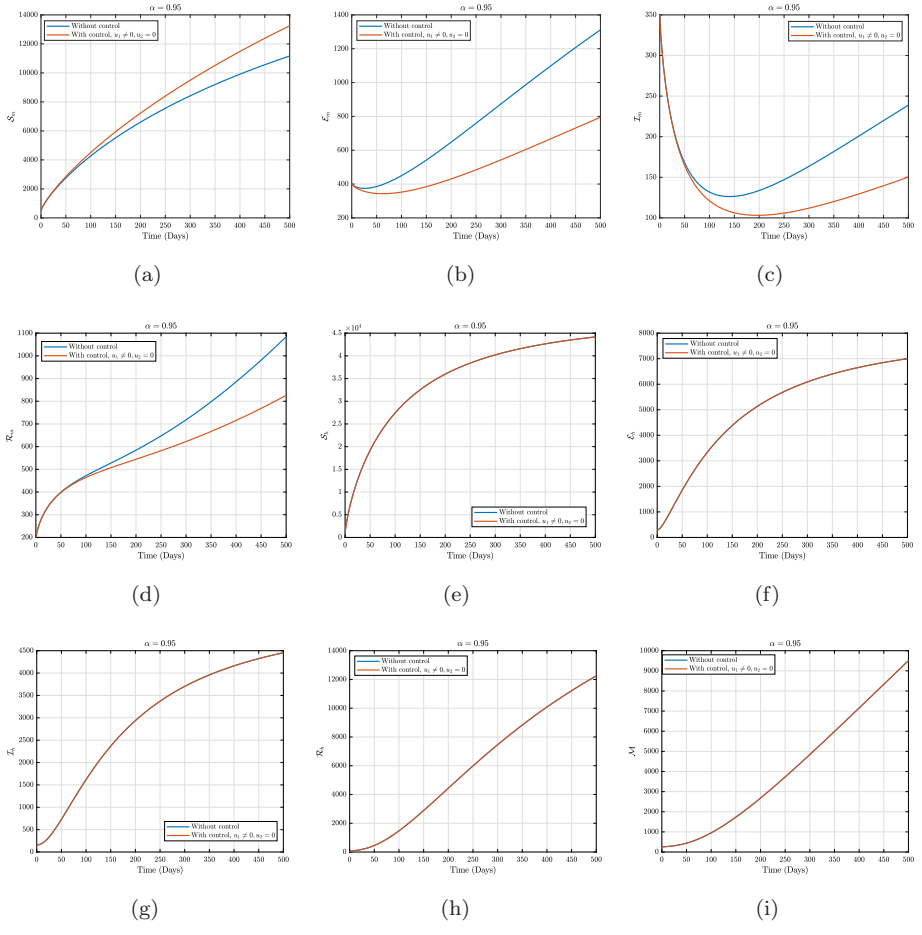

Fig. 6. Effects of varying values of u_1 keeping $u_2 = 0$ on the dynamics of the Mpox at fractional-order value $\alpha = 0.95$. (a) susceptible $\mathcal{S}_\mathfrak{m}$, (b) exposed or latent $\mathcal{E}_\mathfrak{m}$, (c) infected $\mathcal{I}_\mathfrak{m}$, (d) recovered $\mathcal{R}_\mathfrak{m}$, (e) susceptible $\mathcal{S}_\mathfrak{h}$, (f) exposed or latent $\mathcal{E}_\mathfrak{h}$, (g) infected $\mathcal{I}_\mathfrak{h}$, (h) recovered $\mathcal{R}_\mathfrak{h}$, (i) M in model. (3.2)

Similarly, Strategy 2, which is Fig. 7, is used to optimize Mpox disease transmission dynamics while neglecting the use of rodents as pet or avoid touching, $u_1(t)$. We observed a high decrease in the number of exposed and infection in human population and no significant impact or effect in rodent population. This dynamics means that personal protection measures to protect oneself in public transportation such as the use of hydro-alcoholic gel and hand-washing with soap and disinfection spray at a time, that is $u_2(t)$ which has nothing to do with Mpox population.

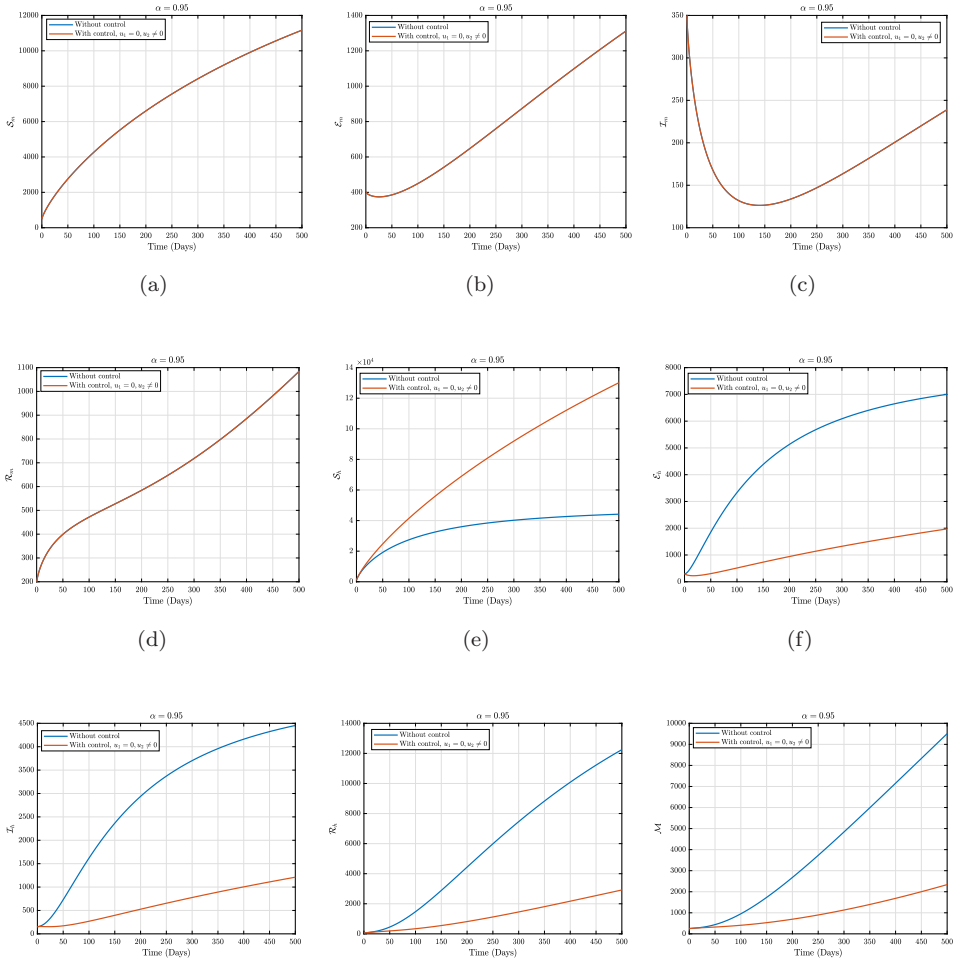

Fig. 7. Effects of varying values of u_2 keeping $u_1 = 0$ on the dynamics of the Mpox fractional-order value at $\alpha = 0.95$ (a) susceptible $\mathcal{S}_\mathfrak{m}$, (b) exposed or latent $\mathcal{E}_\mathfrak{m}$, (c) infected $\mathcal{I}_\mathfrak{m}$, (d) recovered $\mathcal{R}_\mathfrak{m}$, (e) susceptible $\mathcal{S}_\mathfrak{h}$, (f) exposed or latent $\mathcal{E}_\mathfrak{h}$, (g) infected $\mathcal{I}_\mathfrak{h}$, (h) recovered $\mathcal{R}_\mathfrak{h}$, (i) $\mathcal{M}$ in model. (3.2)

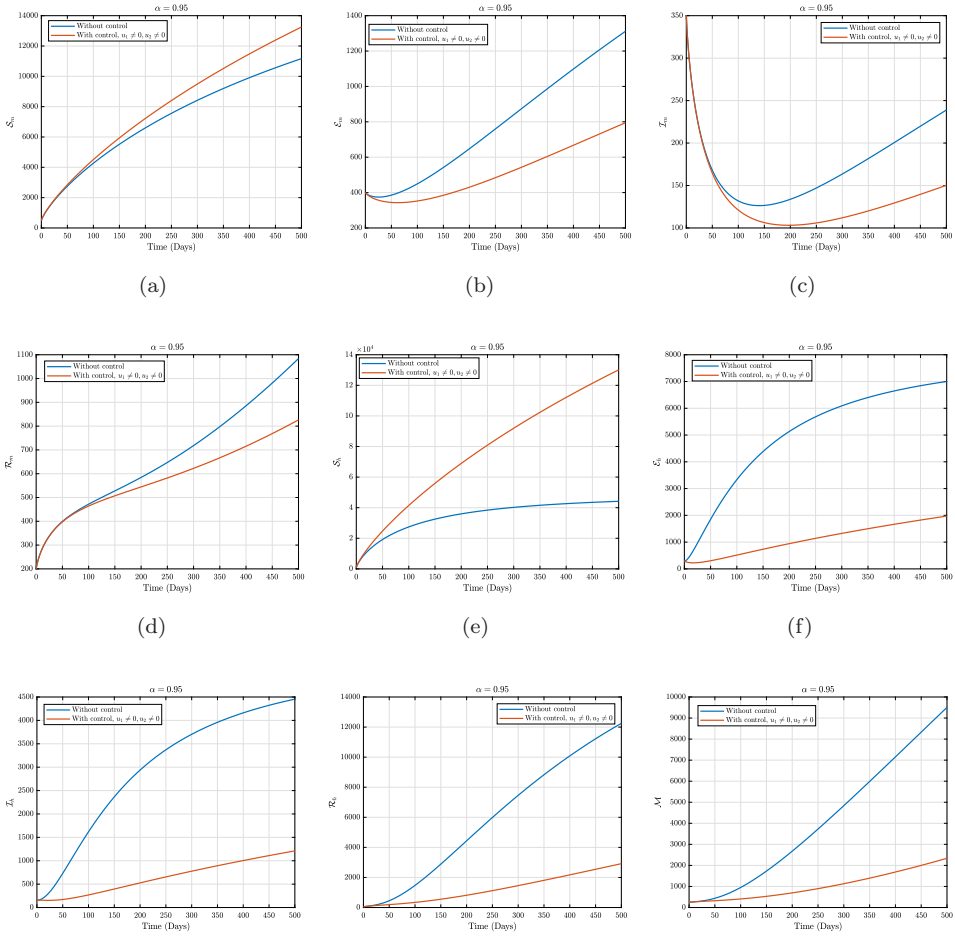

Fig. 8. Effects of varying both the values of u_1 and $u_2 = 0$ on the dynamics of the Mpox at $\alpha = 0.95$. (a) susceptible $\mathcal{S}_\mathfrak{m}$, (b) exposed or latent $\mathcal{E}_\mathfrak{m}$, (c) infected $\mathcal{I}_\mathfrak{m}$, (d) recovered $\mathcal{R}_\mathfrak{m}$, (e) susceptible $\mathcal{S}_\mathfrak{h}$, (f) exposed or latent $\mathcal{E}_\mathfrak{h}$, (g) infected $\mathcal{I}_\mathfrak{h}$, (h) recovered $\mathcal{R}_\mathfrak{h}$, (i) $\mathcal{M}$ in model. (3.2).

Finally, Strategy 3, which is Fig. 8, is used to optimize Mpox disease transmission dynamics. We applied combination of personal protection measures to protect oneself in public transportation and avoidance of touching or using rodents as pets at a time, that are $u_1(t)$ and $u_2(t)$. We observed a significant decrease in the number of exposed and infection in both population as well as transmission through public transport.

7. Conclusion

The impact of control strategies on Mpox disease transmission through our fractional-order mathematical model yields promising results, providing critical

insights into the effectiveness of various intervention measures. The model incorporates two key control strategies: $u_1(t)$ represents practicing avoidance of rodent touch or using rodents as pets at a time, and $u_2(t)$ represents practicing physical distancing and disinfection spray in public transportation. Our numerical simulations demonstrate that the implementation of personal protection measures of avoidance of rodent touch or using rodents as pets at a time, significantly reduces the transmission rates of Mpox disease. Additionally, the adoption of personal protection measures of practicing physical distancing and disinfection spray in public transportation proves effective in controlling the spread of the virus.

However, the most substantial impact on mitigating the burden of Mpox disease is observed when individuals consistently apply a combination of personal protection measures $u_1(t)$ and $u_2(t)$ to prevent disease transmission. This integrated approach demonstrates synergistic effects, leading to a more significant reduction in the overall disease transmission rates. Our findings underscore the importance of individual behaviors in public transport efforts in controlling the spread of both diseases. Adherence to personal protection measures, irrespective of the targeted pathogen, plays a crucial role in limiting transmission and protecting vulnerable populations. Furthermore, the results emphasize the value of comprehensive public transport interventions that address Mpox disease transmission. The application of a fractional-order mathematical model in this study provides a more nuanced understanding of the Mpox infection dynamics.

In conclusion, the insights gained from our study contribute to the development of targeted and efficient control strategies for the Mpox disease infection. By promoting the consistent use of personal protection measures and integrated public transport interventions, public transport authorities can make substantial progress in reducing the transmission and impact of Mpox diseases. These findings highlight the significance of a multidisciplinary approach in combating the Mpox disease infection, ultimately improving global health outcomes and saving lives.

Statements and Declarations

Competing Interest: The writers state that they do not have any competing interests.

CRediT Authorship Contribution Statement: All authors read and approved the final paper.

Data Availability Statement: No data used.

ORCID

Nan Zhang https://orcid.org/0000-0003-1755-116X
Addai Emmanuel https://orcid.org/0000-0003-2159-6299
Mary Nwaife Mezue https://orcid.org/0009-0003-8751-592X

Saima Rashid https://orcid.org/0000-0001-7137-1720
Abiola Akinnubi https://orcid.org/0000-0002-1388-3290
Zalia Abdul-Hamid https://orcid.org/0000-0001-5437-5594
Joshua Kiddy K. Asamoah https://orcid.org/0000-0002-7066-246X

References

[1] T. Khan *et al.*, A mathematical model for the dynamics of SARS-CoV-2 virus using the Caputo–Fabrizio operator, *Math. Biosci. Eng.* **18**(5) (2021) 6095–6116.
[2] K. Rajagopal *et al.*, A fractional-order model for the novel coronavirus (COVID-19) outbreak, *Nonlinear Dynam.* **101** (2020) 711–718.
[3] S. Ahmad *et al.*, Fractional order mathematical modeling of COVID-19 transmission, *Chaos Solitons Fractals* **139** (2020) 110256.
[4] COVID-19 pandemic in Pakistan (2020), http://covid.gov.pk/ (accessed 29 May 2020).
[5] W. Lio and B. Liu, Initial value estimation of uncertain differential equations and zero-day of COVID-19 spread in China, *Fuzzy Optim. Decis. Mak.* **20** (2021) 177–188.
[6] Monkeypox cases confirmed in England — latest updates, UK Health Security Agency (2022), https://www.gov.uk/government/news/monkeypox-cases-confirmed-in-england-latest-updates (accessed 29 August 2022).
[7] E. Mathieu, F. Spooner, S. Dattani, H. Ritchie and M. Roser, Mpox (monkeypox), Our World Data (2022), https://ourworldindata.org/monkeypox (accessed 28 August 2022).
[8] E. Nakayama and M. Saijo, Animal models for Ebola and Marburg virus infections, *Front. Microbiol.* **4** (2013) 267.
[9] R. A. Weinstein *et al.*, Reemergence of monkeypox: Prevalence, diagnostics, and countermeasures, *Clin. Infect. Dis.* **41**(12) (2005) 1765–1771.
[10] I. Arita *et al.*, Human monkeypox: A newly emerged orthopoxvirus zoonosis in the tropical rain forests of Africa, *Am. J. Trop. Med. Hyg.* **34**(4) (1985) 781–789.
[11] Z. Jezek *et al.*, Human monkeypox: A study of 2,510 contacts of 214 patients, *J. Infect. Dis.* **154**(4) (1986) 551–555.
[12] Z. Jezek *et al.*, Human monkeypox: Confusion with chickenpox, *Acta Trop.* **45**(4) (1988) 297–307.
[13] D. L. Heymann, M. Szczeniowski and K. Esteves, Re-emergence of monkeypox in Africa: A review of the past six years, *Br. Med. Bull.* **54**(3) (1998) 693–702.
[14] F. M. Allehiany *et al.*, Mathematical modeling and backward bifurcation in monkeypox disease under real observed data, *Results Phys.* **50** (2023) 106557.
[15] B. Li et al., Aggregation-induced emission-based macrophage-like nanoparticles for targeted photothermal therapy and virus transmission blockage in Monkeypox, *Adv. Mater.* **36** (2023) 2305378.
[16] A. El-Mesady, A. Elsonbaty and W. Adel, On nonlinear dynamics of a fractional order monkeypox virus model, *Chaos Solitons Fractals* **164** (2022) 112716.
[17] Q. Luo and J. Han, Preparedness for a monkeypox outbreak, *Infect. Med.* **1** (2022) 124–134.
[18] E. Sandra, P. Martin and M. Hermann, Zoonotic poxviruses, *Vet. Microbiol.* **140**(3) (2010) 229–236.
[19] World Health Organization, Policy brief on vaccination against monkeypox in the WHO European Region, Policy Brief No. 2, World Health Organization, Regional Office for Europe (2022).

[20] B. R. Akondi and H. B. Ponnam, Monkeypox virus, a global health emergency declared by the world health organization, *Asian J. Pharm. Res. Health Care* **14**(3) (2022) 125.
[21] Molybdenum prices have rallied and risen after interval of 2 months-policy to strengthen regulations for exports by Chinese government has given favorable impression, The TEX Report (2010).
[22] D. Muley *et al.*, Role of transport during outbreak of infectious diseases: Evidence from the past, *Sustainability* **12**(18) (2020) 7367.
[23] H. C. Li, R. Peng and Z. A. Wang, On a diffusive susceptible–infected–susceptible epidemic model with mass action mechanism and birth-death effect: Analysis, simulations, and comparison with other mechanisms, *SIAM J. Appl. Math.* **78**(4) (2018) 2129–2153.
[24] C. K. Manzira, A. Charly and B. Caulfield, Assessing the impact of mobility on the incidence of COVID-19 in Dublin City, *Sustainable Cities Soc.* **80** (2022) 103770.
[25] J. Liu and Y. Zhou, Global stability of an SIRS epidemic model with transport-related infection, *Chaos Solitons Fractals* **40**(1) (2009) 145–158.
[26] E. Addai, A. Adeniji, O. J. Peter, J. O. Agbaje and K. Oshinubi, Dynamics of age-structure smoking models with government intervention coverage under fractal-fractional order derivatives, *Fractal Fract.* **7**(370) (2023) 370.
[27] N. Yousefi, Exploring machine learning methods for predicting disease progression in colon cancer patients (2021), https://etd.adm.unipi.it/t/etd-06102021-163040/.
[28] N. B. Noor, N. Yousefi, B. Spann and N. Agarwal, Comparing toxicity across social media platforms for COVID-19 Discourse, in *Proceeding of the Ninth International Conference on Human and Social Analytics (HUSO 2023)* (Barcelona, Spain, 2023), https://www.thinkmind.org/index.php?view=instance&instance=HUSO+2023.
[29] M. Shaik, N. Yousefi, N. Agarwal and B. Spann, Evaluating role of Instagrams multimedia in connective action leveraging diffusion of innovation and cognitive mobilization theories: Brazilian and Peruvian social unrest case studies, in *2023 10th Int. Conf. Behavioural and Social Computing* (*BESC*), Larnaca, Cyprus, 2023, pp. 1–6, doi:10.1109/BESC59560.2023.10386436.
[30] K. DiCicco, N. B. Noor, N. Yousefi, M. Maleki, B. Spann and N. Agarwal, Toxicity and networks of COVID-19 discourse communities: A tale of two social media platforms, in *Proceedings of the 3rd Workshop on Reducing Online Misinformation through Credible Information Retrieval 2023, co-located with The 45th European Conference on Information Retrieval (ECIR 2023)* (Dublin, Ireland, 2023), http://CeurWs. Org ISSN (1613), p. 0073.
[31] N. Yousefi, N. B. Noor, B. Spann and N. Agarwal, Towards developing a measure to 12 assess contagiousness of toxic tweets, in *Workshop Proceedings of the 17th International AAAI Conference on Web and Social Media, TrueHealth 2023: Workshop on Combating 13 Health Misinformation for Social Wellbeing* (Limassol, Cyprus, 2023), https://doi.org/10.36190/2023.43.
[32] A. D. Zewdie and S. Gakkhar, An epidemic model with transport-related infection incorporating awareness and screening, *J. Appl. Math. Comput.* **68**(5) (2022) 3107–3146.
[33] I. Podlubny, *Fractional Differential Equations*, Mathematics in Science and Engineering (Academic Press, New York, 1999).
[34] A. A. Kilbas, H. M. Srivastava and J. J. Trujillo, *Theory and Applications of Fractional Differential Equations* (Elsevier, Amsterdam, 2006).
[35] D. Guo and V. Lakshmikantham, *Nonlinear Problems in Abstract Cones* (Academic Press, San Diego, 1988).

[36] V. Lakshmikantham and A. S. Vatsala, Basic theory of fractional differential equations, *Nonlinear Anal.* **69**(8) (2008) 2677–2682.
[37] S. Akter and Z. Jin, A fractional order model of the COVID-19 outbreak in Bangladesh, *Math. Biosci. Eng.* **20** (2023) 2544–2565.
[38] I. A. Baba and B. Ghanbari, Existence and uniqueness of solution of a fractional order tuberculosis model, *Eur. Phys. J. Plus* **134** (2019) 1–10.
[39] C. J. Silva and D. F. M. Torres, Stability of a fractional HIV/AIDS model, *Math. Comput. Simul.* **164** (2019) 180–190.
[40] N. Zhang *et al.*, Fractional modeling and numerical simulation for unfolding Marburg–Monkeypox virus co-infection transmission, *Fractals* **31** (2023) 2350086.
[41] M. Ghani *et al.*, A fractional SEIQR model on diphtheria disease, *Model. Earth Syst. Environ.* **9**(2) (2023) 2199–2219.
[42] M. Ngungu *et al.*, Mathematical epidemiological modeling and analysis of monkeypox dynamism with non-pharmaceutical intervention using real data from United Kingdom, *Front. Public Health* **11** (2023) 1101436.
[43] O. J. Peter *et al.*, Fractional order mathematical model of monkeypox transmission dynamics, *Phys. Scripta* **97**(8) (2022) 084005.
[44] E. Addai *et al.*, Modelling the impact of vaccination and environmental transmission on the dynamics of monkeypox virus under Caputo operator, *Math. Biosci. Eng.* **20**(6) (2023) 10174–10199.
[45] O. J. Peter *et al.*, Transmission dynamics of Monkeypox virus: A mathematical modelling approach, *Model. Earth Syst. Environ.* **8** (2022) 3423–3434.
[46] E. Addai *et al.*, Fractional order epidemiological model of SARS-CoV-2 dynamism involving Alzheimer's disease, *Healthcare Anal.* **2** (2022) 100114.
[47] L. Zhang et al., Fractional-order Ebola-Malaria coinfection model with a focus on detection and treatment rate, *Comput. Math. Methods Med.* **2022** (2022) 6502598.
[48] E. Addai *et al.*, A fractional order age-specific smoke epidemic model, *Appl. Math. Model.* **119** (2023) 99–118.
[49] P. Yadav *et al.*, Fractional-order modelling and analysis of diabetes mellitus: Utilizing the Atangana–Baleanu Caputo (ABC) operator, *Alex. Eng. J.* **81** (2023) 200–209.
[50] O. J. Peter *et al.*, Fractional order of pneumococcal pneumonia infection model with Caputo Fabrizio operator, *Results Phys.* **29** (2021) 104581.